Bioorganic Chemistry 134 (2023) 106428

Contents lists available at ScienceDirect

Bioorganic Chemistry

journal homepage: www.elsevier.com/locate/bioorg

Design, synthesis, modeling studies and biological evaluation of pyrazole derivatives linked to oxime and nitrate moieties as nitric oxide donor selective COX-2 and aromatase inhibitors with dual anti-inflammatory and anti-neoplastic activities

Wael A. A. Fadaly [a], Yaseen A. M. M. Elshaier [b], Mohamed T. M. Nemr [c], Khaled R. A. Abdellatif [a,d,*]

[a] Pharmaceutical Organic Chemistry Department, Faculty of Pharmacy, Beni-Suef University, Beni-Suef 62514, Egypt
[b] Organic and Medicinal Chemistry Department, Faculty of Pharmacy, University of Sadat City, Menufya, Egypt
[c] Pharmaceutical Organic Chemistry Department, Faculty of Pharmacy, Cairo University, Kasr El-Eini street 11562, Cairo, Egypt
[d] Pharmaceutical Sciences Department, Ibn Sina National College for Medical Studies, Jeddah 21418, Saudi Arabia

ARTICLE INFO

Keywords:
Anti-inflammatory
Pyrazole
Nitric oxide donor
Cyclooxygenase-2 inhibitors
Anti-neoplastic
Aromatase inhibitors
Molecular docking
Cell cycle analysis
Apoptosis
Conformational isomers
Geometrical aldoxime isomers

ABSTRACT

Two new series of pyrazole derivatives **10a-f** and **11a-f** with selective COX-2 inhibition pharmacophore and oxime/nitrate moieties as NO donor moiety were designed, synthesized and tested for anti-inflammatory, cytotoxic activities and NO release. Compounds **10c**, **11a**, **11e** were more selective for COX-2 isozyme (S.I. = 25.95, 22.52 and 21.54 respectively) in comparison to celecoxib (S.I. = 21.41). Regarding anti-cancer activity, all synthesized compounds were screened by the **National Cancer Institute (NCI)**, **Bethesda, USA** for anticancer activity against 60 human cancer cell lines representing the following cancer types: leukemia, non-small cell lung, colon, CNS, melanoma, ovarian, renal, prostate, and breast cancers. Compounds **10c**, **11a**, **11e** were found to be the most potent inhibitors on breast, ovarian and melanoma cell lines (MCF-7, IGROV1 and SK-MEL-5), compound **11a** causing 79 % inhibition in case of MCF-7, 78.80 % inhibition in case of SK-MEL-5 and unexpected cell growth −26.22 % inhibition in case of IGROV1 (IC_{50} = 3.12, 4.28, 4.13 μM respectively). On the other hand, compounds **10c** and **11e** showed lower inhibition on the same cell lines with IC_{50} = 3.58, 4.58, 4.28 μM respectively for **10c**, IC_{50} = 3.43, 4.73, 4.43 μM respectively for **11e**. Furthermore, DNA-flow cytometric analysis showed that compound **11a** induces cell cycle arrest at G2/M phase leading to cell proliferation inhibition and apoptosis. Additionally, these derivatives examined against F180 fibroblasts to investigate their selectivity indexes. The pyrazole derivative with internal oxime **11a** was the most potent compound against most used cell lines especially MCF-7, IGROV1 and SK-MEL-5 (IC_{50} = 3.12, 4.28, 4.13 μM respectively) with 4.82-fold selectivity towards MCF-7 than F180 fibroblasts. Moreover, oxime derivative **11a** showed potent aromatase inhibitory activity (IC_{50} 16.50 μM) when compared with reference compound letrozole (IC_{50} 15.60 μM). All compounds **10a-f** and **11a-f** released NO in a slow rate (0.73–3.88 %) and the six derivatives **10c**, **10e**, **11a**, **11b**, **11c** and **11e** were the highest NO releasers (3.88, 2.15, 3.27, 2.27, 2.55 and 3.74 % respectively). Herein structure based and ligand based studies were implemented to under stand and evaluate the compounds activity for further in vivo and preclinical studies. Docking mode of final designed compounds with celecoxib (ID: 3LN1) represented that their triazole ring adopted as the core aryl in Y shaped structure. Regarding aromatase enzyme inhibition, docking was carried out with ID: 1 M17. The internal oxime series was more active as anticancer because of their ability to form extra HBs with receptor cleft.

* Corresponding author at: Department of Pharmaceutical Organic Chemistry, Faculty of Pharmacy, Beni-Suef University, Beni-Suef 62514, Egypt.
E-mail address: khaled.ahmed@pharm.bsu.edu.eg (K. R. A. Abdellatif).

https://doi.org/10.1016/j.bioorg.2023.106428
Received 8 December 2022; Received in revised form 1 February 2023; Accepted 12 February 2023
Available online 18 February 2023

1. Introduction

Breast cancer is one of the most common causes of death in women worldwide. Estrogens play an important role in pathogenesis and development of the hormone-dependent (estrogen-receptor positive or ER +) breast cancer [1]. Aromatase is the key rate-limiting enzyme that responsible for conversion of androgens to estrogens [1]. Recently, there are two drug categories used for treatment of hormone-dependent breast cancer, drugs acting on the estrogen receptor (selective estrogen receptor modulators) and drugs that block activity of the aromatase enzyme (aromatase inhibitors or AIs) [1]. The inhibition of aromatase enzyme activity is preferable choice to decrease the amount of estrogen production without affecting the production of other steroids in the estrogen biosynthetic pathway [1]. AIs can be classified into steroidal as **formestane** and nonsteroidal aromatase inhibitors as **anastrozole (1)**, **letrozole (2)** and **vorozole (3)** and **MS4** as dual aromatase-steroid sulfatase inhibitors based on a biphenyl template, Fig. 1. Depending on their mechanisms of action, steroidal AIs are androstenedione analogs which interact irreversibly to the active site of the aromatase whereas nonsteroidal AIs bind to the aromatase active site reversibly [2,3]. In general, NSAIs have azole ring system attached to aromatic structures in Y-shape manner. Heterocyclic nitrogen atom has an important role for NSAIs structure-activity relationship as it interacts with heme iron of the P450 enzymes which inhibit hydroxylation reactions for aromatization [4]. Other parts of the structure interact with the apoprotein moiety of the active binding site on the aromatase enzyme. Aromatase inhibitors include azole derivatives containing imidazole ring such as fadrozole (4) together with derivatives containing 1,2,4-triazole ring such as anastrozole (1), letrozole (2) and vorozole (3) [5]. The effect of 1,2,3-triazole instead of 1,2,4-triazole has been examined in the letrozole structure [6]. It has shown that the position of the nitrogen atom in either position 3 or 4 of the 1,2,4 triazole is important for good inhibition of aromatase. The derivatives containing triazole ring are used as first-line NSAIs, and they are all well tolerated, selective and highly effective. The most effective aromatase inhibitor is letrozole (2); it can inhibit 99 % of the aromatase enzyme in peripheral tissues [5]. Some studies have shown that the selectivity of NSAIs can be increased by the change of the triazole system with azole bioiso

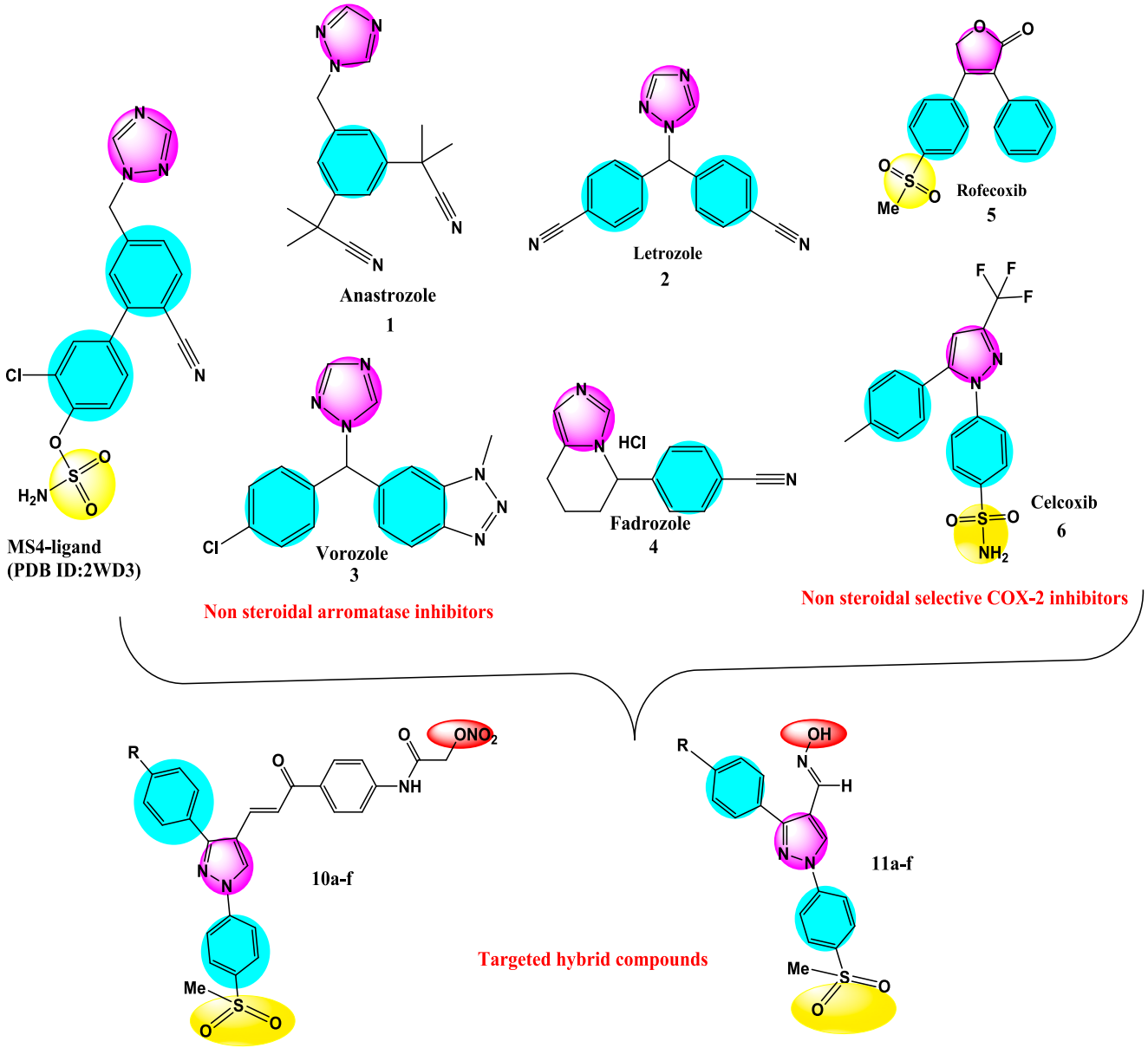

Fig. 1. Nonsteroidal anti-aromatase drugs, celecoxib, rofecoxib and designed compounds.

steres and also by enhancing the aromatic structures in the side chain [6].

Recent evidence shows that commonly prescribed drugs, such as non-steroidal anti-inflammatory drugs (NSAIDs) may have beneficial roles in the primary chemoprevention of breast cancer as there is a significant relationship between aromatase (CYP19) and cyclooxygenase-2 (COX-2) expression in cancerous tissues. In the breast, PGEs increase aromatase activity therefore COX-2 inhibition has been shown to prevent estrogen-dependent breast cancer [7]. COX-2 directly regulates gene expression of specific aromatase promoter regions and regulates aromatase activity so agents that inhibit COX-2 or block the biological effects of PGE2 may be useful in significantly limiting aromatase activity and proliferation of human breast tumor cells. [8] In addition, PGE2 derived from cyclooxygenase, increases intracellular cAMP levels and stimulates estrogen biosynthesis and decrease aromatase mRNA expression and enzyme activity in breast cancer cells. [7,9,10] Epidemiological studies revealed that non-steroidal anti-inflammatory drugs (NSAIDs) especially rofecoxib (5), [11] celecoxib (6), [11] indomethacin [12] have been shown to reduce the risk of breast cancer [13]. Celecoxib and rofecoxib were prescribed in breast cancer due to their action to regulate the level of aromatase inhibitors in a clinical study. [11,14,15].

On the other hand, nitric oxide (NO) plays an essential role in both inflammation and cancer process. During inflammation, nitric oxide (NO) protects digestive system from ulceration by increasing of the mucosal blood flow due to its vasodilation effect. In addition, NO enhances the response of the mucosal immune system and increase the healing of an ulcerated mucosal cell. [16–20] According to the above-mentioned findings, to overcome the NSAIDs associated side effects of either non-selective or selective COX-2 inhibitors, hybrid of NSAID possessing a NO-donor moiety (NO-NSAID) has been emerged [21–27]. In addition, during cancer it was observed that nitric oxide had a dual effect in the breast cancer phenotype sensitive to estrogen-induced apoptosis. Nitric oxide, at low concentration, the nanomolar level, induced cell growth, great metabolism and downregulation of estrogen receptor and enhanced collective invasion, leading to a more violent phenotype. On contrary, higher nitric oxide concentrations (100 nM) prevents cell growth, metabolism and promotes apoptosis. [28] One of the most essential roles of NO in treatment of cancer is blocking of aromatase both by reducing mRNA for the enzyme and by direct inhibition of enzyme activity as a result of the formation of a nitrosothiol on the cysteine moiety neighboring to the heme in aromatase enzyme. [29] In addition, it was reported that NO inhibits estradiol secretion independent of cGMP by inhibiting P450 aromatase activity in cultured porcine granulosa cells PGC. [30] In addition to extend the study on human granulosa cells, ovarian granulosa-luteal cells gained from female experiencing in-vitro fertilization (IVF) were utilized and it was found that the action of NO is due to the down-regulation of aromatase gene transcription. Although NO reduced intracellular cAMP values, down-regulation of aromatase gene transcription may not be arbitrated by protein kinase A-dependent mechanisms. [31].

Pyrazole derivatives are one of the most exciting moieties showing high anti-inflammatory activity. [32–37] It was reported that 1,3,4-trisubstituted-pyrazole derivatives as lonazolac analogs were synthesized and evaluated for their anti-inflammatory activity, it was found that it possessed promising COX-2 selectivity, anti-inflammatory activity and gastric safety profile. [32] In addition, 1,5diarylpyrazole derivatives were synthesized and were significantly less ulcerogenic when compared to ibuprofen and celecoxib. [33] A series of pyrazole bearing an oxime NO donor moiety was prepared and tested for their anti-inflammatory and anti-cancer activities and it showed outstanding cell proliferation inhibition activity against the tested cell lines. [38–40] (Fig. 1).

Based on the aforementioned data and as a continuation of our research interest in the scope of synthesis and biological evaluation of celecoxib analogs, [32–35,41] celecoxib-NO hybrids [36–38] and antineoplastic agents and apoptotic inducer, [42–45] we aimed to study the effect of combination of the three bioactive entities, in order to accomplish novel selective COX-2 inhibitors lacking complications associated with the prolonged use of non-selective COX inhibitors (NSAIDs) [46–52] and get an improved gastrointestinal safety when compared to the traditional NSAIDs. [53–58] We targeted the Y shaped structure design of COX-2 selective coxibs with their bioactive pharmacophores (SO_2NH_2) or (SO_2CH_3) which are important for COX-2 selectivity with pyrazole ring which is azole bioisostere with anti-cancer aromatase inhibition activity with or without a linker in our designed structure hybrid between the coxib pyrazole core and a tail containing oxime or nitrate moieties as NO donor in one compact structure hybrid for the purpose of synergism the anti-inflammatory activity and minimizing the both expected ulcerogenic and cardiovascular side effects of coxibs and also we hope these hybrids will show additional anti-cancer aromatase inhibition activity. Consequently, we now describe the synthesis, *in vitro* evaluation as COX-1/ COX-2 inhibitors, *in vitro* anti-cancer activity, cell cycle analysis, apoptosis and NO release studies for two new series of pyrazole/ NO donor hybrid **10a-f**, and **11a-f**. The target derivatives **10a-f** and **11a-f** had some modifications in the structure of celecoxib (5) including; (i) aryl alkyl linker was incorporated in pyrazole C-4 of celecoxib analogues **10a-f** or omitted in celecoxib analogues **11a-f**. (ii) The Y-shaped design with central pyrazole core of celecoxib was maintained in both series **10a-f** and **11a-f** as azole bioisostere of common AIs to achieve aromatase inhibition activity. (iii) Amino sulfonyl (SO_2NH_2) group in phenyl moiety at pyrazole C-1 was replaced with methane sulfonyl moiety (SO_2Me) in **10a-f** and **11a-f** this replacement is expected to maintain COX-2 selectivity, since the proposed compounds have COX-2 pharmacophore (SO_2Me or SO_2NH_2), (iv) The trifluoro methyl group in C-3 of celecoxib was replaced with its para substituted aryl group in both series **10a-f** and **11a-f** to achieve the Y shape of structure of the target hybrid COX-2/ aromatase inhibitor, (v) The nitrate NO donor moiety was incorporated as a tail part in aryl alkyl linker in series 8a-f and oxime NO donor moiety was directly attached to pyrazole C-4 in series **11a-f**. (Fig. 1).

2. Results and discussion:

2.1. Chemistry

The chalcone derivatives **(8a-f)** were prepared via condensation of the appropriate reported heteroaldehydes **(7a-f)** [59] with *p*-amino-acetophenone in ethanolic sodium hydroxide. Furthermore, upon alkylation of the prepared chalcones **(8a-f)** with chloroacetylchloride afforded the *N*-substituted acetamide derivatives **(9a-f)** which upon nucleophilic substitution with silver nitrate in acetonitrile gave the oxoethyl nitrate **(10a-f)** as nitric oxide donor derivatives. In addition formation of the other nitric oxide donor oxime series **11a-f** was synthesized upon treatment of the appropriate reported hetero aldehydes **(7a-f)** with hydroxyl amine hydrochloride in acetonitrile and in the presence of catalytic amount of sodium acetate (Scheme.).

The structures of the newly synthesized compounds **10a-f** & **11a-f** were confirmed by their spectral IR, ^1H, ^{13}C NMR, mass and elemental analyses. The ^1H NMR spectra of derivatives **10a-f** showed a singlet signal corresponding to $SO_2\underline{CH_3}$ group at δ 3.29–3.37 ppm. Additionally, compounds **10a,b** showed a phenomenon of geometrical isomerization around alkene C═C double bond and that resulted in presence of two geometrical isomers *E* & *Z* for compounds **10a,b** which announced for duplication of all proton signals in ^1H NMR spectra for these two compounds and appearance of two *J* values for both olifinic protons of the two geometrical isomers as 14.8–16.0 *Hz* for *E* isomer and 8.4 *Hz* for *Z* isomer with ratio of *1: 0.2* for *E/Z* isomers respectively and that was clear in the ^1H NMR spectra which showed presence of two singlet signals of methylene group adjacent to the nitrate moiety at 4.33, 5.14 ppm and two single peaks for pyrazole H-5 at 9.28–9.29, 9.55–9.58 ppm with the same ratio *1: 0.2* due to *E/Z* isomers respectively.

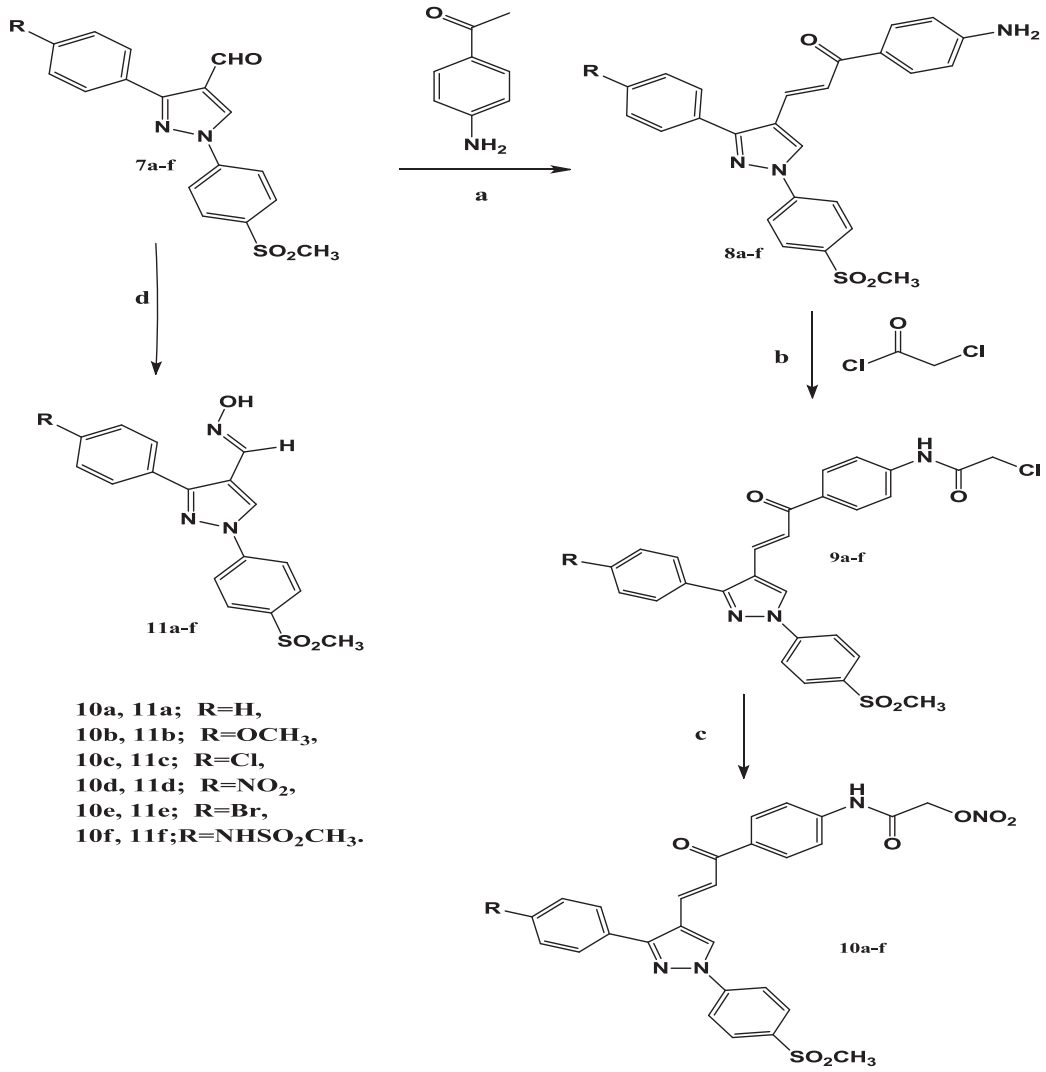

Scheme 1. Reagents and conditions. a) NaOH / ethanol, stirring room temperature 24 h, b) DMF stirring room temperature 24 h, c) acetonitrile, $AgNO_3$, reflux 8 h, d) acetonitrile, $NH_2OH.HCl$, sodium acetate, reflux 8 h.

Furthermore, compound **10c** showed no geometrical isomerism and that was clear from appearance of only one *J* value for olifinic protons as 15.6 *Hz* indicating existence of only *E* isomer and there was no duplication of aromatic protons signals or pyrazole H-5 signal which appeared as one singlet signal at 9.56 ppm but compound **10c** showed a phenomenon of conformational isomerism resulted in restriction of free rotation around the N—C amidic bond. Rotomers are conformational isomers where interconversion by rotation around a single bond is restricted. [60] As a result aliphatic methylene (CH_2) attached to nitrate moiety in derivative **10a** appeared as two singlet signals with two protons total integration at δ 4.33, 5.28 ppm (which due to splitting into two singlets at two different chemical shifts but their integration equals 2H due to free rotation around amidic N—C bond between the amidic NH atom and the carbonyl carbon. In addition, the amidic NH proton signal in ^{1}H NMR was splitted into two singlet peaks at δ 10–11 ppm but with total one proton integration due to existence of two conformers in derivatives **10a**.

In addition, presence of bulky phenyl para substituents as nitro, bromo and 4-(methylsulfonamido) groups in derivatives **10d-f** restricted these derivatives in the most stable *staggered* conformer and *E* geometrical isomer and resulted in disappearance of both geometrical or conformational isomerism and existence of these derivatives **(10d-f)** as one *E/staggered* isomer due to stability of both and restriction of free rotation and that was cleared from ^{1}H NMR spectra which showed no duplication of any of aromatic protons or CH_2 peak which was appeared as one singlet peak at 5.27–5.28 ppm or pyrazole H-5 which was appeared as one singlet signal at 9.58–9.61 ppm respectively. In addition of appearance of only one *J* value of olifinic protons as 15.2 *Hz*.

The ^{1}H NMR spectra of derivatives **11a-f** showed a singlet signal corresponding to SO_2CH_3 group at δ 3.29 ppm. On the other hand, aldoximes **11a,b,c** existed as *syn* & *anti* geometrical isomer at minor and major ratios respectively and that was clear in their ^{1}H NMR spectrum through duplication of all the signals of these compounds for example, aldoxime proton appears as two unequal singlet signals at δ 7.43–7.46 & 8.12–8.14 ppm due to syn & anti isomers in integration ratio as 1:1/5, 1:1/2 and 1:1/5 respectively in compounds **11a,b,c**. In addition, pyrazole H-5 appears as two unequal singlet signals at δ 8.98–9.33 ppm due to syn & anti isomers with the same previous proton ratio. Furthermore, the hydroxyl proton of aldoxime appeared as two singlet signals at δ 11.19–11.98 ppm due to syn & anti isomers with typical mentioned proton ratio as well as signals of aromatic protons and SO_2CH_3 group were duplicated with the same ratio. As aromatic protons corresponding to phenyl moiety attached to pyrazole C-3 appeared at δ 7.55–7.74 ppm two overlapped doublets due to syn & anti isomers. As well as, two doublets corresponding to 4-methanesulfonylphenyl protons (H-2, H-6) & (H-3, H-5) appeared at δ 8.08–8.27 ppm also duplicated.

In contrast, aldoximes **11d,e,f** not showed the phenomenon of existence of two geometrical isomers in ^{1}H NMR but they were present as

one geometrical isomer and not showed duplication of the aldoxime protons, pyrazole H-5 and aldoxime hydroxyl proton signals and that due to the existence of bulky groups para substituents as nitro, bromo and 4-(methylsulfonamido) groups which restricted these derivatives in the most stable *anti* geometry.

A 2D NOESY experiment was done for compounds **11a-c** beside the 1D ^{1}H NMR in order to show correlations between spatially close protons. Correlations between the two singlets SO_2CH_3 protons of the two geometrical syn & anti-aldoximes and the OH proton of both their syn & anti-aldoxime (**11a-c**) supports our assumption that the orientation of the SO_2CH_3 group is in a position capable of be near to aldoxime OH group and also the existence of two compounds as a mixture of geometrical isomers. **(**Figs. 2a-c**).**

Trial was done to separate **11c** two geometrical isomers using **Biotage Isolera One Flash Chromatograph** (Column Type: Biotage® Sfär HC Duo 5 g and Flow Rate: 5 ml/min) (System Information Software: SELEKT 1.3.2–11737 Instrument ID: AAA-BCJ-JAI-GAJ) at Research Institute of Medicinal & Aromatic Plants, Beni-Suef University. **(**Fig. 3**).**

The chromatogram showed the separation of two bands of the two geometrical isomer and the two crops were collected using hexane as an eluent and the major crop was identified by ^{1}H NMR which showed **the separation of only one isomer** with one aldoxime proton at 7.41 ppm and one pyrazole H-5 at 9.65 ppm.

2.2. Biological evaluation

2.2.1. In-vitro anti-inflammatory activity

The *in vitro* COX-1/COX-2 inhibition was determined using COX-1 Inhibitor Screening Kit-K548 (Biovision, S. Milpitas Blvd., Milpitas, CA 95035 USA) and COX-2 Inhibitor Screening Kit-K547 (Biovision, S. Milpitas Blvd., Milpitas, CA 95035 USA) to monitor the isozyme-specific inhibition. The potency of testing compounds was determined as the concentration causing 50 % enzyme inhibition (IC_{50}). The results (Table 1) showed that compounds **10c, 10d, 10e, 11a, 11b, 11c, 11e, 9f** had good inhibitory activities against COX-1 isozyme (IC_{50} = 5.18–8.18 μM range). On the other hand, Compounds **10b, 10c, 10e, 11a, 11e** exhibited high COX-2 isozyme inhibitory activities (IC_{50} = 0.20–0.39 μM range). From the above results, we can conclude that compounds **10c**, **11a**, **11e** have both excellent COX-1/COX-2 inhibition with highest COX-2 selectivity indexes in the range of 25.95 to 21.54 in comparison with the COX-2 selective reference drug celecoxib (COX-1 IC_{50} = 8.78 μM, COX-2 IC_{50} = 0.41 μM and S.I. = 21.41).

2.2.2. In-vitro anticancer screening

All synthesized compounds were selected (except compound **10d** which was declined) by the National Cancer Institute (NCI), Bethesda, USA for anticancer screening against 60 human cancer cell lines representing the following cancer types: leukemia, colon, non-small cell lung, melanoma, CNS, renal, ovarian, prostate, and breast cancers. A single dose (10^{-5} M) screening was carried out and the cells were incubated for 48 h. End point determination was carried out using Sulforhodamine-B (SRB) as protein dye. The percent inhibition was calculated, and the results were represented (see the supplementary data).

2.2.3. In vitro cytotoxicity IC_{50} determination

Compounds **10c**, **11a** and **11e** were further evaluated by determining the IC_{50} against breast, ovarian and melanoma cell lines (MCF-7, IGROV1 and SK-MEL-5) by the MTT colorimetric assay using doxorubicin as a reference compound [61]. IC_{50} of compounds **10c**, **11a**, **and 11e** was determined and compared to the IC_{50} of doxorubicin (Figure 2). Compound **11a** showed excellent inhibitory activity (with IC_{50} = 3.12 (MCF-7), 4.28 (SK-MEL-5), 4.13 (IGROV1) μM) compared to doxorubicin (with IC_{50} = 2.97 (MCF-7), 3.38 (SK-MEL-5), 3.70 (IGROV1) μM).

2.2.4. Flow cytometry analysis

Cell cycle analysis of compound **11a** compared to doxorubicin as a reference compound were tested against breast cell line MCF-7 at their IC_{50} concentrations, changes in the cell cycle phases were noted upon adding compound **11a** on breast MCF-7 cells (Fig. 3). It was noted that there was a decrease in the percentage of apoptotic cells at the pre-G phase (26.17 % when treated with **11a** and 14.52 % for doxorubicin) in comparison to the control (2.18 %). The percentage of cells at G0/G1 was decreased to 31.54 % in comparison to the control which showed 57.05 %. While treating the same cells with doxorubicin caused incomparable reduction in G0-G1 (37.61 %). Concerning the S phase, compound **11a** was capable of inducing lower reduction in the percentage of the cell to (23.78 %) than doxorubicin (31.46 %) compared to the control (31.82 %). On the other hand, when treating breast cells MCF-7 with compound **11a**, a dramatic increase in cells at G2/M phase was occurred to (44.68 %) than control (11.13 %) and higher than that of doxorubicin (30.93 %). According to these results, it can be concluded that compound **11a** showed cell cycle arrest at G2/M phase leading to

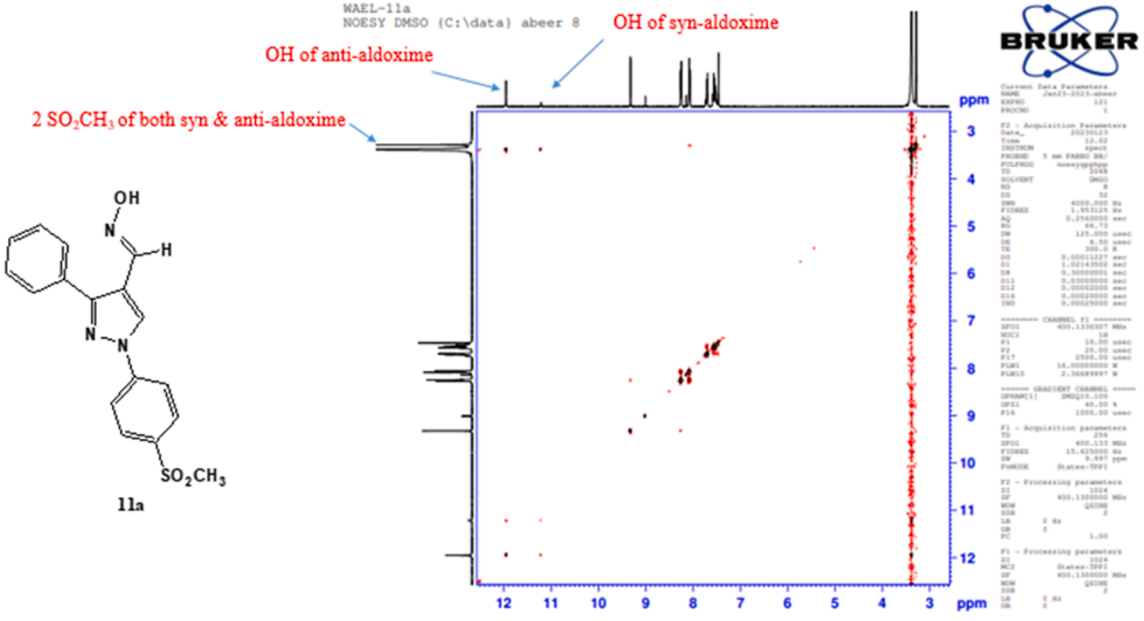

Fig. 2a. 2D NOSEY of compound 11a showing existence of two geometrical syn & anti-aldoximes.

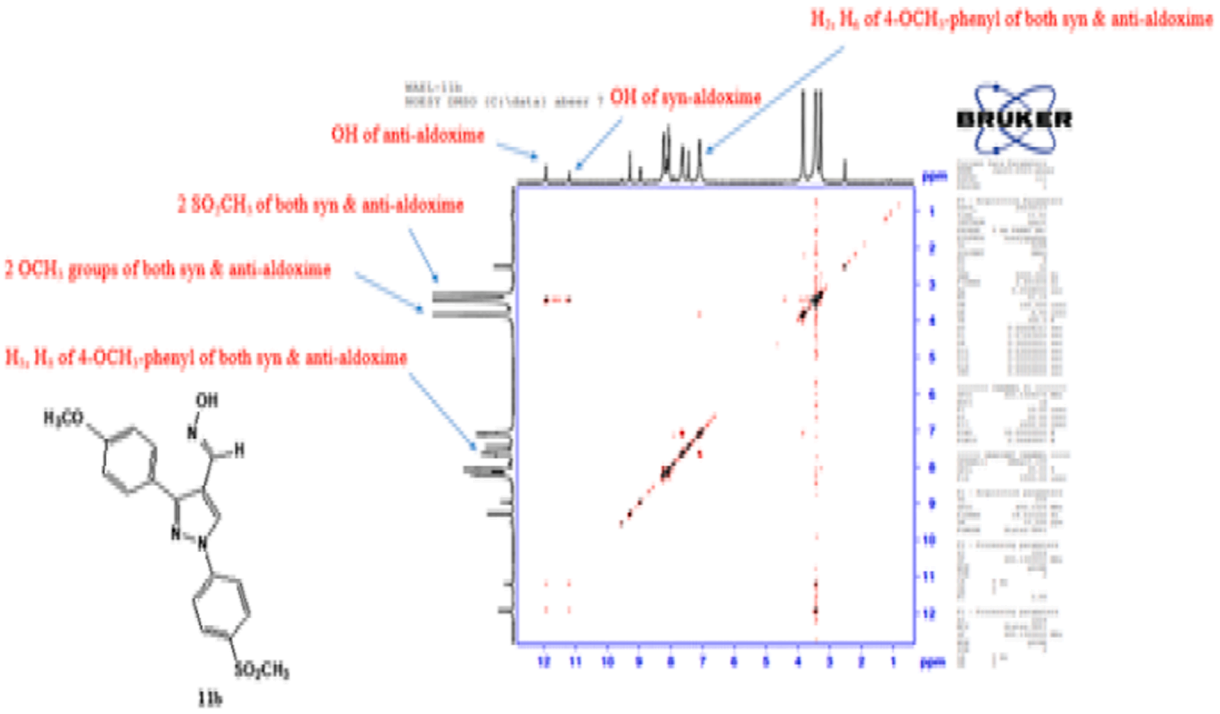

Fig. 2b. 2D NOSEY of compound 11b showing existence of two geometrical syn & anti-aldoximes.

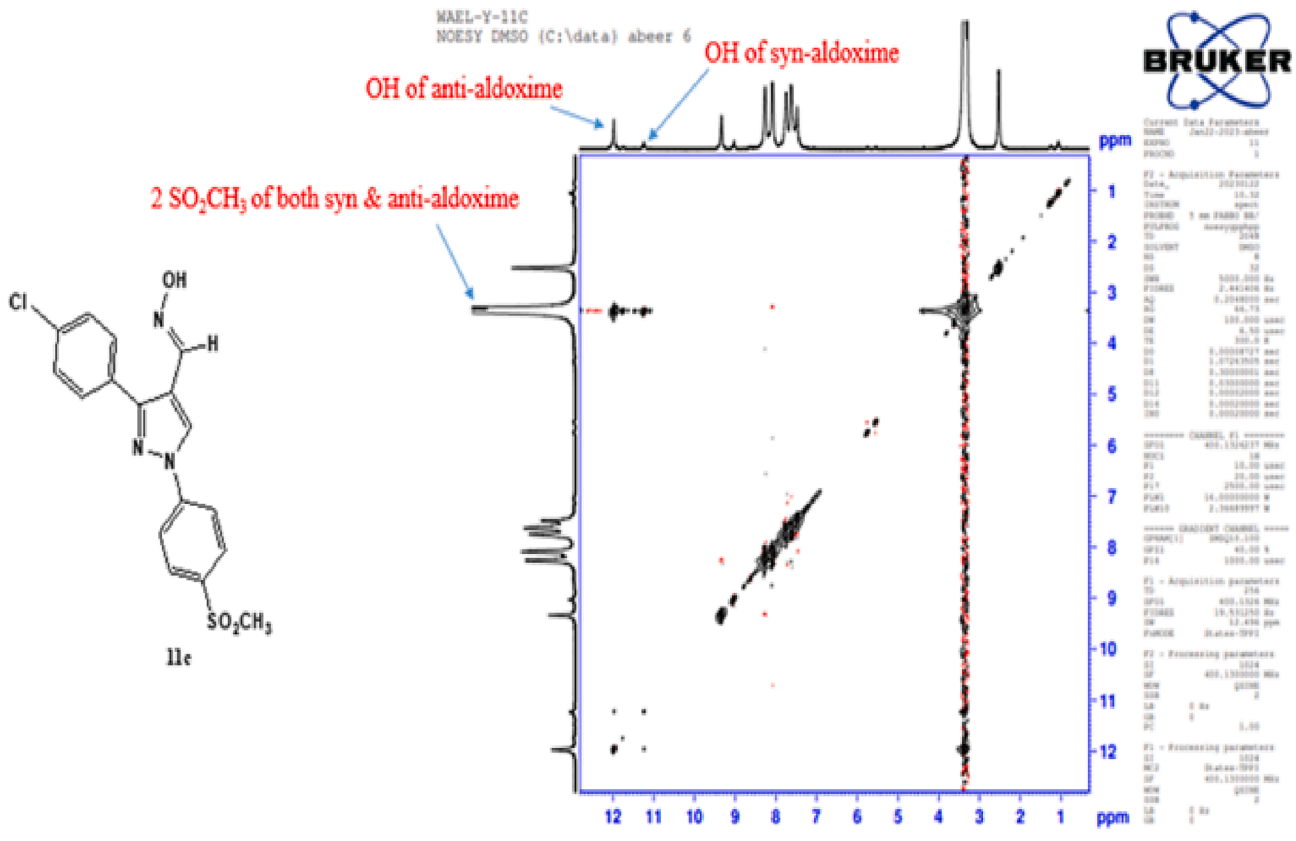

Fig. 2c. 2D NOSEY of compound 11c showing existence of two geometrical syn & anti-aldoximes.

cell proliferation inhibition and apoptosis.

2.2.5. *Determination of apoptosis using annexin-V*

Treatment of MCF-7 breast cells with compound **11a** resulted in an increase in annexin-V positive apoptotic cells at the early and late apoptotic stages with 9.41 % (10.2 fold) and 14.18 % (61.6 fold) respectively, whereas for doxorubicin 6.51 % (7.0 fold) and 6.18 % (26.8 fold) increase in early and late apoptosis respectively compared to

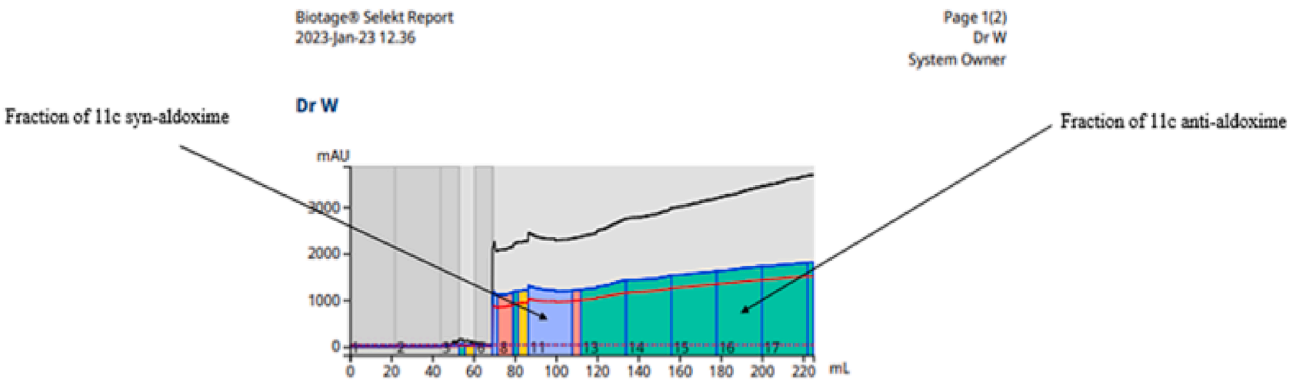

Fig. 3. Flash column chromatogram of compound 11c showing existence of two geometrical syn & anti-aldoximes.

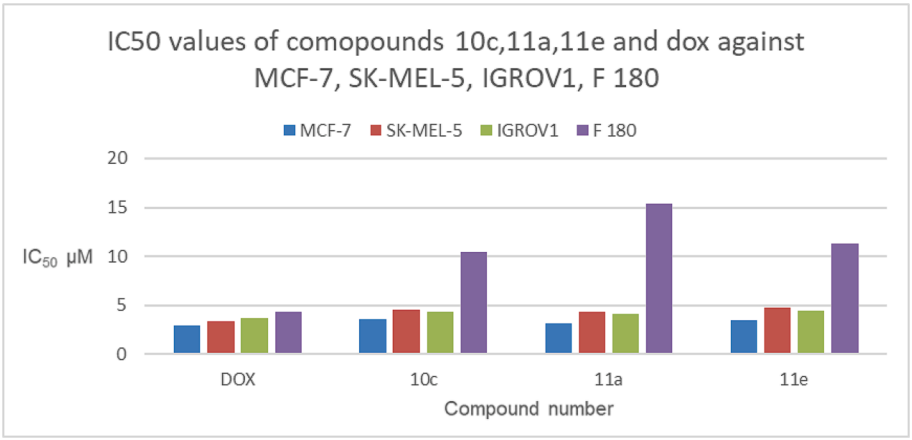

Fig. 4. Bar presentation graph representing IC_{50} of compounds **10c**, **11a** and **11e** compared to reference doxorubicin against MCF-7, SK-MEL-5, IGROV1 and F180 cell lines.

control (0.92 % and 0.23 % respectively). Furthermore, compound **11a** and doxorubicin induced a necrotic percentage of 2.58 % and 1.83 %, respectively which were considerably higher than control that showed only 1.03 % necrosis (Fig. 6).

2.2.6. *Aromatase inhibitory activity*

Aromatase inhibitory activity of compounds **10c, 11a and 11e** was determined using Aromatase (CYP19A) inhibitor screening Kit. Five concentrations were used and the determination of IC_{50} was carried out using letrozole as reference. The results showed that compound **10c, 11a and 11e** induced strong inhibitory activity against aromatase with IC_{50} of 20.1, 16.50 and 21.5 μM respectively which was comparable to that of letrozole (IC_{50} = 15.60 μM).

2.3. *Nitric **oxide release***

The percent of NO released from the prepared compounds **10a-f** and **11a-f** was determined through incubation in phosphate-buffered-saline (PBS at pH 7.4) (see data in Table 2). All compounds **10a-f** and **11a-f** released NO in a slow rate (0.73–3.88 %). where nitrate derivatives **11a-f** have higher NO release rate than oxime derivatives **8a-f**. Moreover, the six derivatives **10c**, **10e**, **11a**, **11b**, **11c** and **11e** were the highest NO releasers (3.88, 2.15, 3.27, 2.27, 2.55 and 3.74 % respectively).

2.4. *Molecular modeling studies:*

2.4.1. *Molecular docking*

2.4.1.1. ***Docking with COX-2 enzyme (PDB: ID 3LN1)*** *[62]*. To validate our docking protocol, docking mode and pose for celecoxib, the co-crystallized ligand, was re docked and compared with its complex form with the receptor. [62] Both structures represented complete overlay with same binding interaction, supplementary file. In comparison to all compounds, compound **11a** docked with the active site with best consensus score 4, celecoxib has 0 consensus score value. This compound exhibited similar binding mode to celecoxib however the overlay as a Y shape (vicinal diaryl pharmacophore) did not detected. The tolyl moiety of celecoxib did not find the similar fragment from compound **11a,** Fig. 5a. Compound **10c**, with consensus score 21, showed good similarity to celecoxib and succeed to form Y shape as celecoxib, however the nitrate acetyl moiety extended deeply inside the receptor, Fig. 7b.

2.4.1.1. ***Docking with aromatase enzyme (PDB:ID:2WD3)*** *[63]*. Compound **10c** occupied the receptor with the formation of different hydrogen bonds (HBs). It illustrated binding mode and pose with a complete overlay with the co-crystallized protein ligand (MS4), Fig. 6a. The co-crystallized ligand formed two HBs with Thr: 198 and HB with Asn: 62A. The methyl sulfonyl functionality of compound **10c** formed strong HB with Thr: 198A. Additionally, the nitrate terminal engaged in HB formation with Arg: 58A. Both compound **10c** and co-crystallized ligand showed complete overlay and similarity in binding mode and pose, Fig. 6a. Interestingly, compound **11a** represented a complete overlay to co-crystallized ligand, Fig. 6b. This candidate formed two HBs with Thr: 198A (as ligand) through methyl sulfonyl group and HB with Asn: 62A through its oxime functionality. Presence of sulfomyl group in compound **11e** changed the compound pose and shifted the group to close the Arg: 58A. It formed two HBs with Thr: 198A, Fig. 8c.

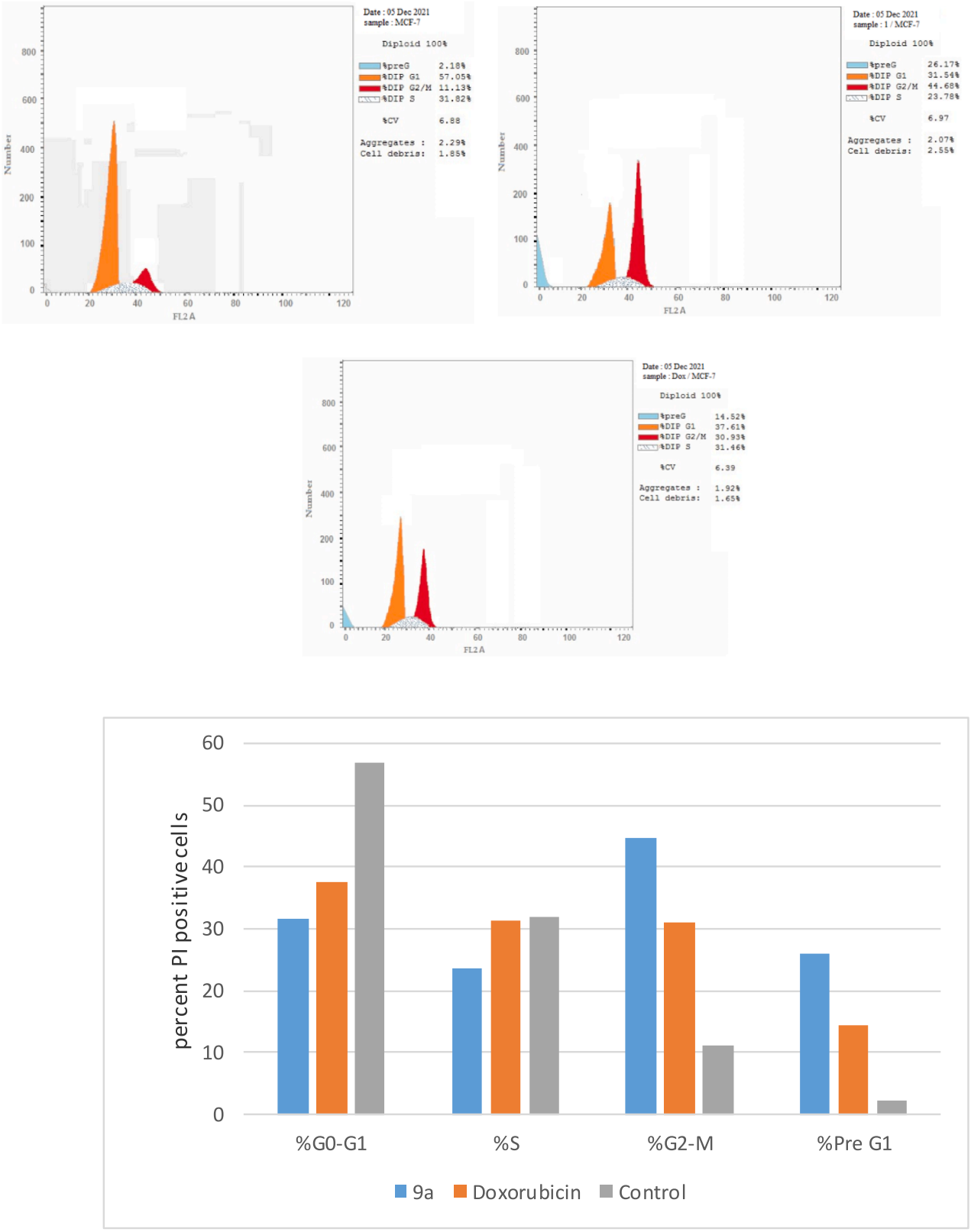

Fig. 5. Compound **11a** effect on DNA-ploidy flow cytometric analysis of breast MCF-7 cells compared to doxorubicin and negative control.

2.4.1.2. Shape alignment and rapid overlay chemical structure (ROCS). The analysis of chemical features for targeted compounds using ROCS analysis was built to figure out the different pharmacophoric features. ROCS technique has different applications in drug discovery and development. [64–66] Herein, the druggabilty parameters and colour atom descriptors [66] were determined by OpenEye program (academic license, Yaseen Elshaier), Table 3 and Fig. 9. From Table 3, comparing compound **10c** with compound **10a**, both of them contain the same number of color atoms and are similar in physicochemical properties however compound **10c** has a higher log P and lower molecular weight.

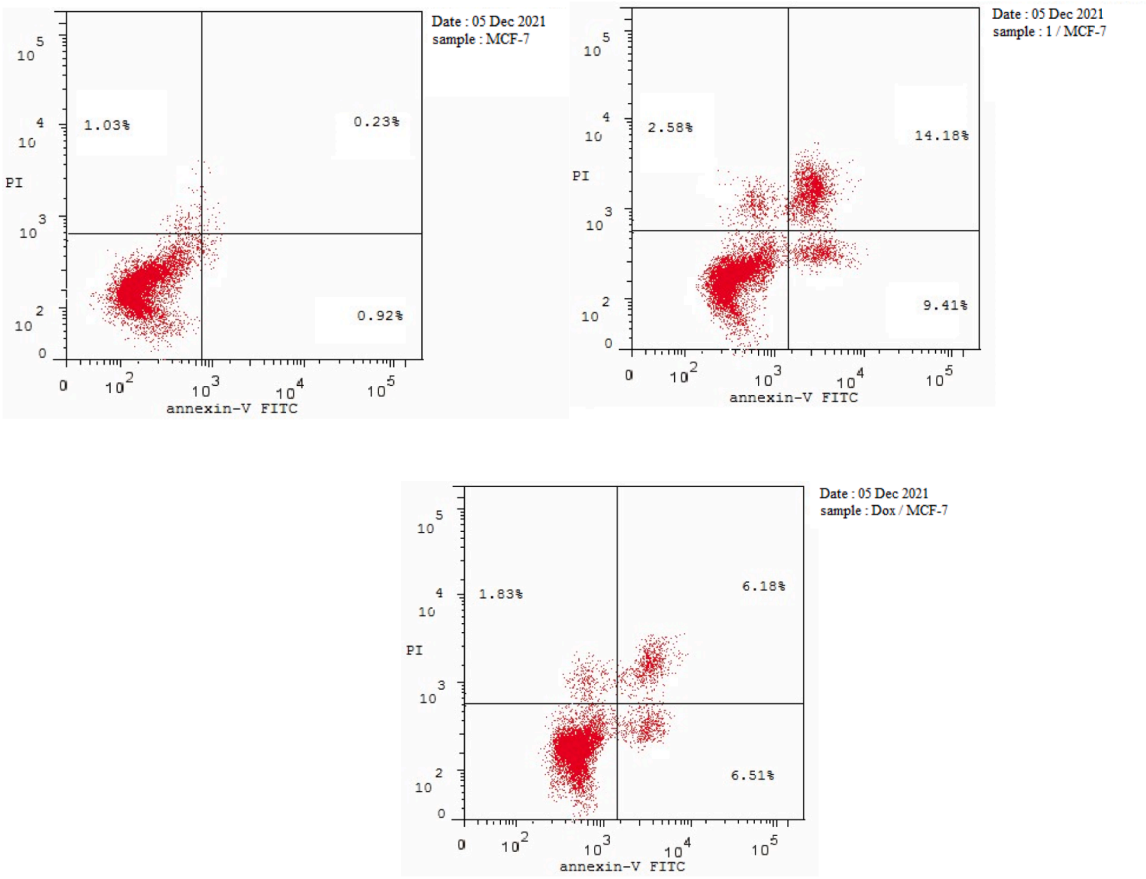

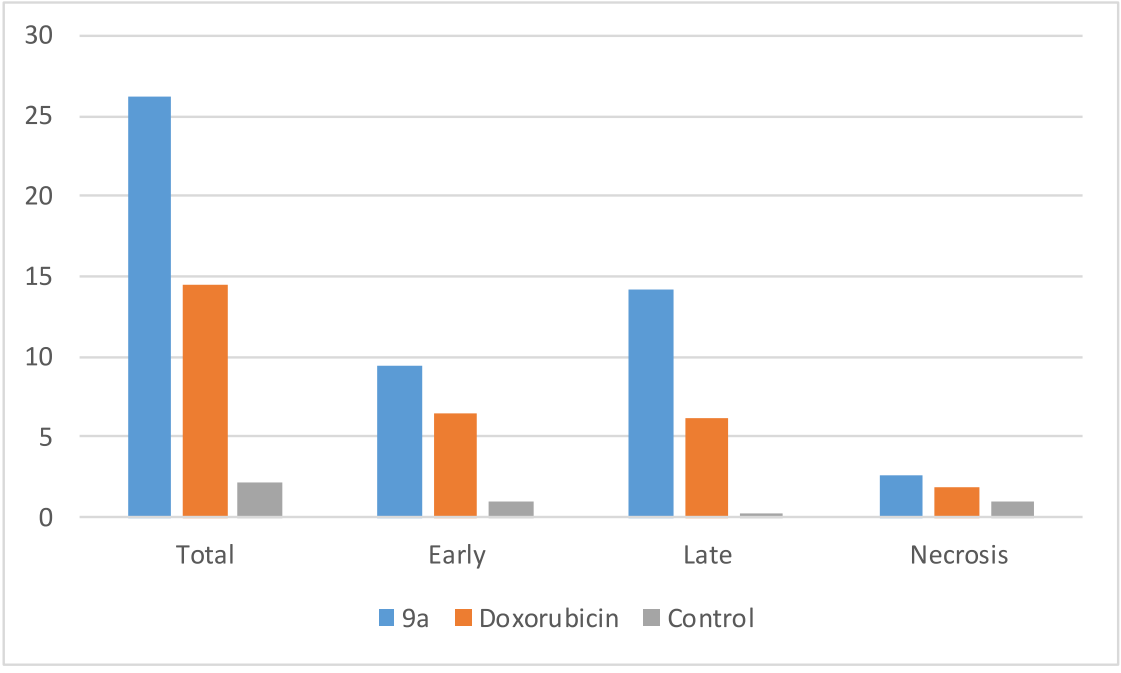

Fig. 6. the percentage of Annexin-V-FITC-positive staining in breast MCF-7 cells when treated with compound **11a** compared to doxorubicin and negative control.

Compound **11a** in comparison to compound **11c**, has lower molecular weight and lower logP and a higher number of heavy atoms.

Shape alignment and shape similarity for designed compounds were determined using ROCS analysis (ROCS application Open Eye scientific software).

The standard aromatase inhibitor (MS4) was selected as a query for comparison. The quantitative determination for compounds similarity based on their 3D structures is calculated by Tanimoto combo score (TC). TC score with value from 0 to 2 and the query take the value 2. of celecoxib (TC 0.85), compound **11a (TC 0.67)**, compound **11e (TC**

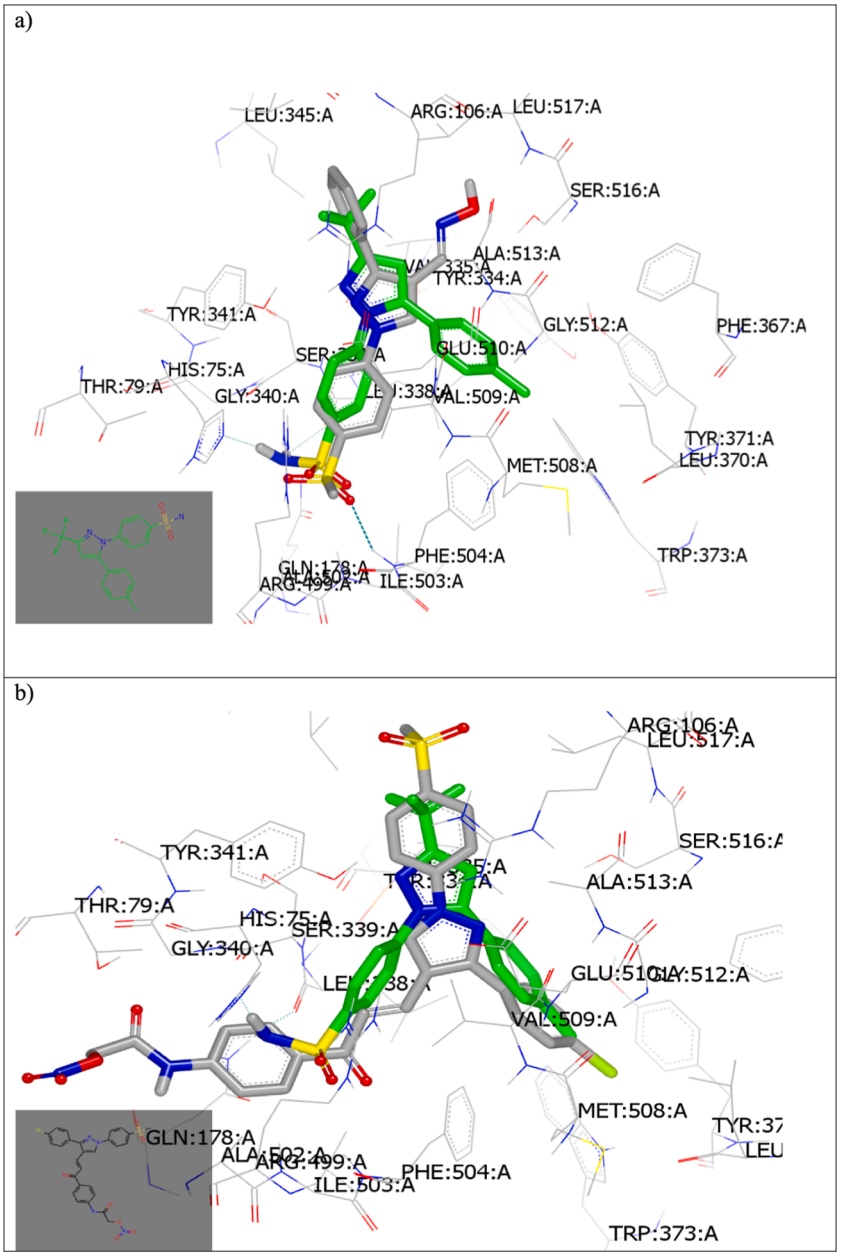

Fig. 7. Visual representation by vida. a) compound **9a** (grey colour) and celecoxib (green colour); b) compound **8c** (grey colour) and celecoxib (green colour) docked with PDBID:3LN1.

0.84) and compound **10c (TC 0.52)** with **MS4** standard aromatase inhibitor (green colour) as a query **(TC 2)**.

3. Conclusion

The results displayed compounds 11a, 11e (TC 0.84) and **10c** very good drug candidate. Compound **11a** represented good druggabilty parameters and which suggested us for further investigation for in vivo and pre clinical studies.

4. Experimental

4.1. Chemistry

General: Melting points were determined on a Thomas-Hoover capillary apparatus and are uncorrected. Infrared (IR) spectra were recorded as films on KBr plates using a Nicolet 550 Series II Magna FT-IR spectrometer. 1H NMR and 13C NMR spectra were measured on a Bruker 400 MHz NMR Spectrophotometer, Faculty of Pharmacy, Beni-Suef University, Egypt in CDCl3 or DMSO-d6 with TMS as the internal standard, where J (coupling constant) values are estimated in Hertz (Hz). Mass spectra (MS) were recorded on a Water's Micromass ZQ 4000 mass spectrometer using the electro-spray (ES) ionization mode. Microanalyses were performed for C, H and N were carried out on Perkin-Elmer 2400 analyzer (Perkin-Elmer, Norwalk, CT, USA) at the Microanalytical unit of Cairo University, Egypt. All compounds were within ± 0.4 % of the theoretical values. Silica gel column chromatography was performed using Merck silica gel 60 ASTM (70–230 mesh). Trials to separate the geometrical isomers of compound 11c was done using Biotage Isolera One Flash Chromatograph at Department of Chemistry of Medicinal and Aromatic Plants, Research Institute of Medicinal & Aromatic plants, Beni-Suef University for providing the analysis work on. Compounds 7a-f were prepared according to the previously reported procedures. [59]

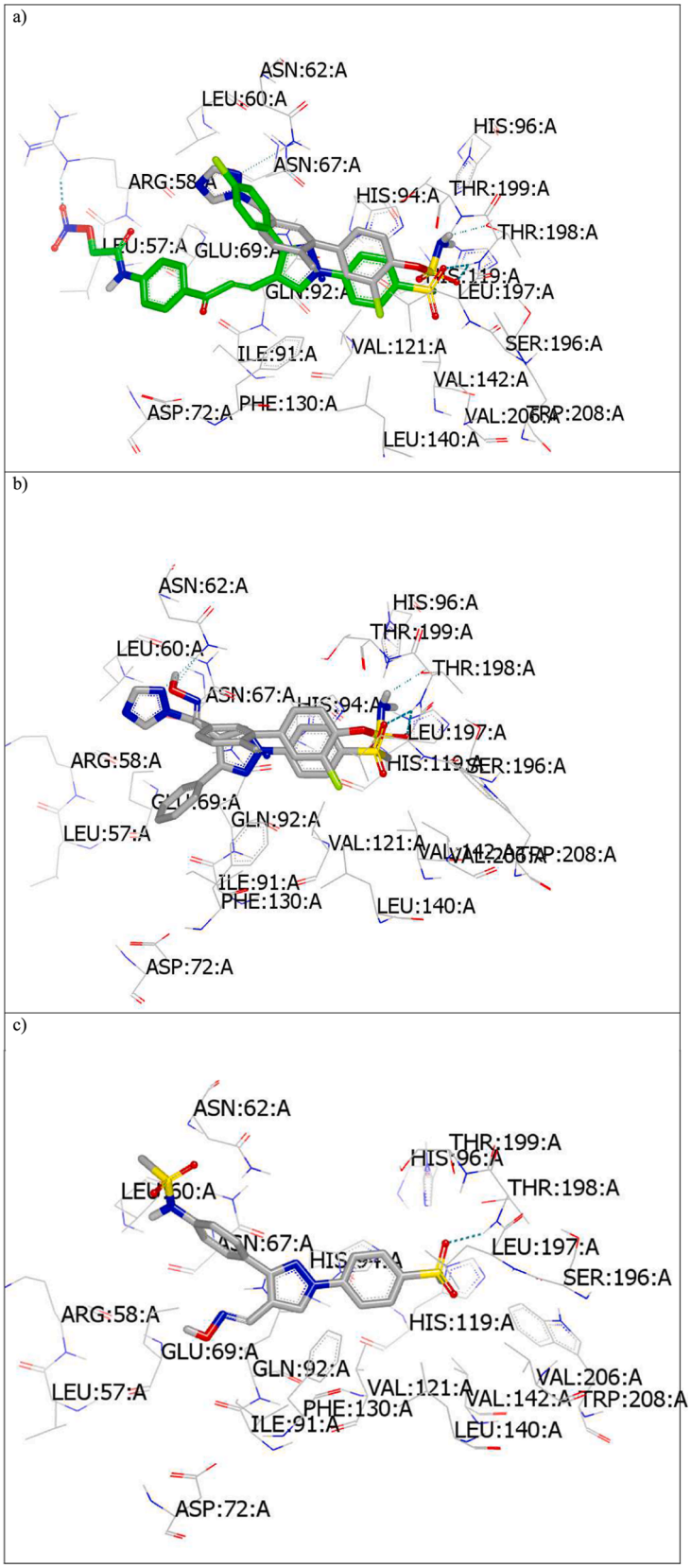

Fig. 8. Visual representation by vida. a) compound **10c** (green colour) and standard ligand (grey colour); b) compound **11a**; and c) compound **11e** docked with PDBID:2WD3.

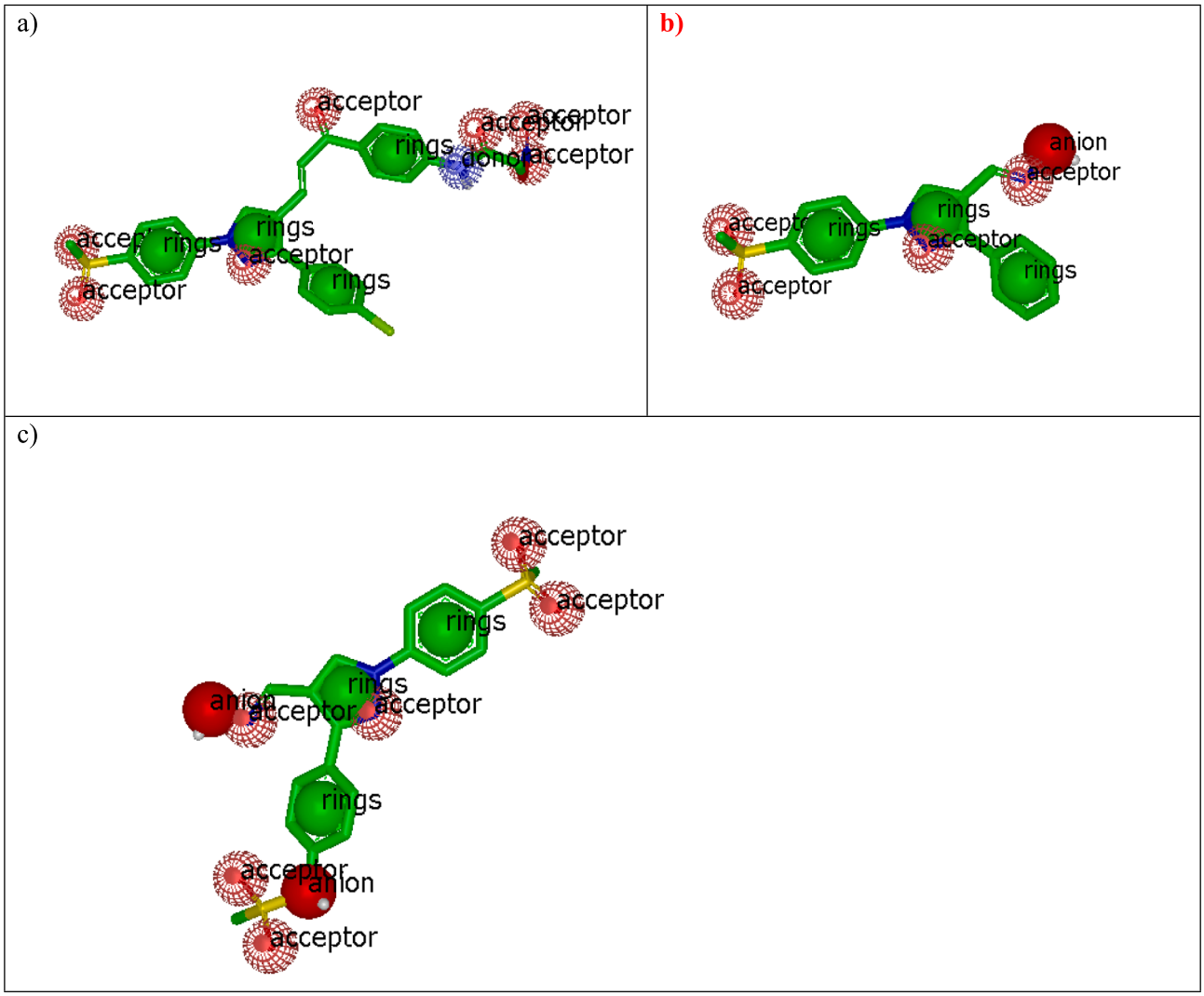

Fig. 9. Colour atoms by ROCS anlysis. a) Compound 10c; b) Compound 11a; c) compound 11e.

4.1.1. General procedure for synthesis of the chalcone derivatives (8a-f):

A mixture of the appropriate pyrazole aldehydes (**5a-f,** 2.0 mmol), 4-amino acetophenone (2.0 mmol) and 10 % aqueous sodium hydroxide (4 ml) in ethanol (30 ml) was stirred at room temperature for 24 h, the resulting formed solid was filtered, dried and crystallized from ethanol to give the final chalcone derivatives (**8a-f**). Physical and spectral data are listed below:

4.1.1.1. (E)-1-(4-aminophenyl)-3-(1-(4-(methylsulfonyl)phenyl)-3-phenyl-1H-pyrazol-4-yl)prop-2-en-1-one (8a). Yield 81 %; yellow solid; m.p. 185–187 °C; IR (KBr): 3472, 3333 (NH_2), 3124 (C═H aromatic), 2923 (C—H aliphatic), 1675 (C═O), 1596 (-C═C-), 1553 (C═N), 1403, 1145 (SO_2CH_3) cm^1; ^{1}H NMR (DMSO-d_6, 400 MHz, δ, ppm): 3.30 (s, 3H, $SO_2\underline{CH_3}$), 6.20 (s, 2H, NH_2, D_2O exchangeable); 6.64 (d, J = 8.0 Hz, 2H, 4-aminophenyl H-3, H-5), 7.52 (d, J = 15.2 Hz, 1H, CH = C olifenic proton H_α), 7.53 (m, 3H, phenyl H-3, H-4, H-5), 7.68 (d, J = 8.0 Hz, 2H, phenyl H-2, H-6), 7.94 (d, 2H, 4-aminophenyl H-2, H-6), 7.96 (d, J = 15.2 Hz, 1H, CH = C olifenic proton H_β), 8.12 (d, J = 8.2 Hz, 2H, 4-methanesulfonylphenyl H-2, H-6), 8.23 (d, J = 8.2 Hz, 2H, 4-methanesulfonylphenyl H-3, H-5), 9.53 (s, 1H, pyrazole H-5); MS *m/z* (ES^+) 443.13 (M +) (100 %). Anal. Calcd. For $C_{25}H_{21}N_3O_3S$: C, 67.70; H, 4.77; N, 9.47; Found; C, 76.96; H, 4.98; N, 9.69.

4.1.1.2. (E)-1-(4-aminophenyl)-3-(3-(4-methoxyphenyl)-1-(4-(methylsulfonyl)phenyl)-1H-pyrazol-4-yl)prop-2-en-1-one (8b). Yield 74 %; yellow solid; m.p. 177–179 °C; IR (KBr): 3441, 3361 (NH_2), 3136 (C═H aromatic), 2917 (C—H aliphatic), 1643 (C═O), 1590 (-C═C-), 1535 (C═N), 1403, 1146 (SO_2CH_3) cm^1; ^{1}H NMR (DMSO-d_6, 400 MHz, δ, ppm): 3.30 (s, 3H, $SO_2\underline{CH_3}$), 3.85 (s, 3H, OCH_3), 6.19 (s, 2H, NH_2, D_2O exchangeable); 6.64 (d, J = 8.0 Hz, 2H, 4-aminophenyl H-3, H-5), 7.07 (d, J = 8.0 Hz, 2H, 4-methoxyphenyl H-3, H-5), 7.13 (d, J = 8.2 Hz, 2H, 4-aminophenyl H-3, H-5), 7.55 (d, J = 15.2 Hz, 1H, CH = C olifenic proton H_α), 7.61 (d, J = 8.0 Hz, 2H, 4-methoxyphenyl H-2, H-6), 7.88 (d, J = 15.2 Hz, 1H, CH = C olifenic proton H_β), 7.92 (d, J = 8.0 Hz, 2H, 4-aminophenyl H-2, H-6), 8.11 (d, J = 8.2 Hz, 2H, 4-methanesulfonylphenyl H-2, H-6), 8.26 (d, J = 8.2 Hz, 2H, 4-methanesulfonylphenyl H-3, H-5), 9.49 (s, 1H, pyrazole H-5); MS *m/z* (ES^+) 473.14 (M +) (100 %). Anal. Calcd. For $C_{26}H_{23}N_3O_4S$: C, 65.94; H, 4.90; N, 8.87; Found; C, 66.32; H, 4.77; N, 8.62.

4.1.1.3. (E)-1-(4-aminophenyl)-3-(3-(4-chlorophenyl)-1-(4-(methylsulfonyl)phenyl)-1H-pyrazol-4-yl)prop-2-en-1-one (8c). Yield 68 %; white solid; m.p. 165–167 °C; IR (KBr): 3439, 3354 (NH_2), 3133 (C═H aromatic), 2921 (C—H aliphatic), 1650 (C═O), 1592 (-C═C-), 1535 (C═N), 1403, 1146 (SO_2CH_3) cm^1; ^{1}H NMR (DMSO-d_6, 400 MHz, δ, ppm): 3.30 (s, 3H, $SO_2\underline{CH_3}$), 6.21 (s, 2H, NH_2, D_2O exchangeable); 6.65 (d, J = 8.0 Hz, 2H, 4-aminophenyl H-3, H-5), 7.52 (d, J = 15.2 Hz, 1H,

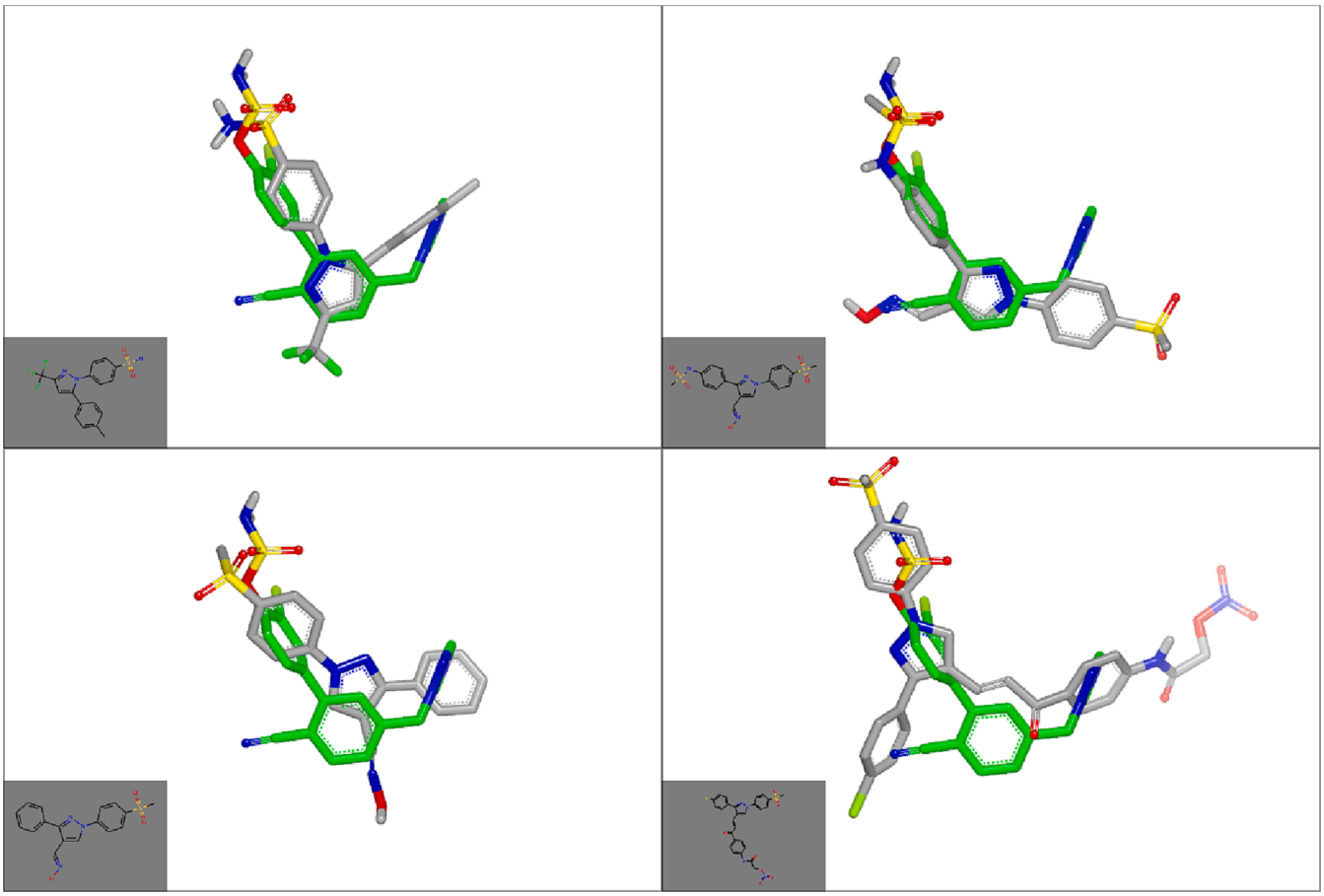

Fig. 10. Visual representation by Vida. Shape alignment by ROCS analysis of celecoxib, compound **11a**, compound **11e** and compound **10c with MS4** standard aromatase inhibitor (green colour) as a query.

Table 1
In vitro COX-1 and COX-2 inhibitory activity of pyrazole derivatives **10a-f**, **11a-f** and reference drug celecoxib.

Compound	COX-1 IC_{50} (μM)[a]	COX-2 IC_{50} (μM)[a]	COX-2 S.I.[b]
10a	8.93	0.42	21.26
10b	8.93	**0.39**	**22.89**
10c	**6.23**	**0.24**	**25.95**
10d	**8.18**	0.47	17.40
10e	**7.73**	**0.20**	**38.65**
10f	20.58	2.58	7.97
11a	**5.18**	**0.23**	**22.52**
11b	**7.88**	0.42	18.76
11c	**7.13**	0.67	10.64
11d	9.08	0.83	10.93
11e	**6.68**	**0.31**	**21.54**
11f	**7.88**	0.44	17.90
Celecoxib	8.78	0.41	**21.41**

[a] The concentration of test compound produce 50% inhibition of COX-1, COX-2 enzyme, the result is the mean of two values. [b] The *in vitro* COX-2 selectivity index (COX-1/COX-2).

CH = C olifenic proton H_α), 7.61 (d, J = 8.0 Hz, 2H, 4-aminophenyl H-3, H-5), 7.69 (d, J = 8.0 Hz, 2H, 4-chlorophenyl H-2, H-6), 7.82 (d, J = 15.2 Hz, 1H, CH = C olifenic proton H_β), 7.87 (d, J = 8.0 Hz, 2H, 4-chlorophenyl H-3, H-5), 8.13 (d, J = 8.0 Hz, 2H, 4-methanesulfonylphenyl H-2, H-6), 8.18 (d, J = 8.0 Hz, 2H, 4-methanesulfonylphenyl H-3, H-5), 9.50 (s, 1H, pyrazole H-5); MS m/z (ES^+) 477.09 (M +) (100 %). Anal. Calcd. For $C_{25}H_{20}ClN_3O_3S$: C, 62.82; H, 4.22; N, 8.79; Found; C, 62.72; H, 4.12; N, 8.55.

Table 2
% of *NO* release of the prepared compounds.

Compound No.	% *NO* released
8a	1.72
8b	1.66
8c	3.88
8d	0.73
8e	2.15
8f	0.95
9a	3.27
9b	2.27
9c	2.55
9d	0.93
9e	3.74
9f	1.73

4.1.1.4. (E)-1-(4-aminophenyl)-3-(1-(4-(methylsulfonyl)phenyl)-3-(4-nitrophenyl)-1H-pyrazol-4-yl)prop-2-en-1-one (8d). Yield 69 %; yellow solid; m.p. 195–197 °C; IR (KBr): 3436, 3334 (NH_2), 3111 (C═H aromatic), 2926 (C—H aliphatic), 1688 (C═O), 1595 (-C═C-), 1526 (C═N), 1405, 1146 (SO_2CH_3) cm^1; ^{1}H NMR (DMSO-d_6, 400 MHz, δ, ppm): 3.30 (s, 3H, $SO_2\underline{CH_3}$), 6.19 (s, 2H, NH_2, D_2O exchangeable); 6.64 (d, J = 8.2 Hz, 2H, 4-aminophenyl H-3, H-5), 7.53 (d, J = 15.2 Hz, 1H, CH = C olifenic proton H_α), 7.60 (d, J = 8.0 Hz, 2H, 4-nitrophenyl H-2, H-6), 7.73 (d, J = 8.2 Hz, 2H, 4-aminophenyl H-2, H-6), 7.82 (d, J = 15.2 Hz, 1H, CH = C olifenic proton H_β), 8.86 (d, J = 8.0 Hz, 2H, 4-nitrophenyl H-3, H-5), 8.13 (d, J = 8.2 Hz, 2H, 4-methanesulfonylphenyl H-3, H-5), 8.27 (d, J = 8.2 Hz, 2H, 4-methanesulfonylphenyl H-2, H-6), 9.52 (s, 1H, pyrazole H-5); MS m/z (ES^+) 488.12 (M +) (100 %). Anal. Calcd. For $C_{25}H_{20}N_4O_5S$: C, 61.47; H, 4.13;

N, 11.47; Found; C, 61.80; H, 4.28; N, 11.64.

4.1.1.5. (E)-1-(4-aminophenyl)-3-(3-(4-bromophenyl)-1-(4-(methylsulfonyl)phenyl)-1H-pyrazol-4-yl)prop-2-en-1-one (8e). Yield 69 %; yellow solid; m.p. 217–219 °C; IR (KBr): 3472, 3371 (NH_2), 3113 (C═H aromatic), 2923 (C—H aliphatic), 1655 (C═O), 1594 (-C═C-), 1536 (C═N), 1400, 1145 (SO_2CH_3) cm^1; ^1H NMR (DMSO-d_6, 400 MHz, δ, ppm): 3.31 (s, 3H, $SO_2\underline{CH_3}$), 6.21 (s, 2H, NH_2, D_2O exchangeable); 6.64 (d, J = 8.2 Hz, 2H, 4-aminophenyl H-3, H-5), 7.52 (d, J = 15.2 Hz, 1H, CH = C olifenic proton H_α), 7.66 (d, J = 8.0 Hz, 2H, 4-bromophenyl H-2, H-6), 7.82 (d, J = 8.2 Hz, 2H, 4-aminophenyl H-2, H-6), 7.86 (d, J = 15.2 Hz, 1H, CH = C olifenic proton H_β), 8.88 (d, J = 8.0 Hz, 2H, 4-bromophenyl H-3, H-5), 8.13 (d, J = 8.2 Hz, 2H, 4-methanesulfonylphenyl H-3, H-5), 8.20 (d, J = 8.2 Hz, 2H, 4-methanesulfonylphenyl H-2, H-6), 9.55 (s, 1H, pyrazole H-5); MS m/z (ES^+) 521.04 (M +) (100 %). Anal. Calcd. For $C_{25}H_{20}BrN_3O_3S$: C, 57.48; H, 3.86; N, 8.04; Found; C, 57.30; H, 3.72; N, 8.38.

4.1.1.6. (E)-N-(4-(4-(3-(4-aminophenyl)-3-oxoprop-1-en-1-yl)-1-(4-(methylsulfonyl)phenyl)-1H-pyrazol-3-yl)phenyl)methanesulfonamide (8f). Yield 66 %; white solid; m.p. 185–187 °C; IR (KBr): 3447, 3368 (NH_2), 3124 (C═H aromatic), 2924 (C—H aliphatic), 1657 (C═O), 1590 (-C═C-), 1533 (C═N), 1400, 1148 (SO_2CH_3) cm^1; ^1H NMR (DMSO-d_6, 400 MHz, δ, ppm): 3.10 (s, 3H, $NHSO_2\underline{CH_3}$), 3.30 (s, 3H, $SO_2\underline{CH_3}$), 5.39 (s, 2H, NH_2, D_2O exchangeable); 6.79 (d, J = 8.0 Hz, 2H, 4-aminophenyl H-3, H-5), 7. 22 (d, J = 15.2 Hz, 1H, CH = C olifenic proton H_α), 7.28 (d, J = 8.0 Hz, 2H, *N*-phenylmethanesulfonamide H-3, H-5), 7.40 (d, J = 8.0 Hz, 2H, *N*-phenylmethanesulfonamide H-2, H-6), 7.61 (d, 2H, 4-aminophenyl H-2, H-6), 7.65 (d, J = 15.2 Hz, 1H, CH = C olifenic proton H_β), 7.66 (d, J = 8.2 Hz, 2H, 4-methanesulfonylphenyl H-2, H-6), 7.71 (d, J = 8.2 Hz, 2H, 4-methanesulfonylphenyl H-3, H-5), 9.56 (s, 1H, pyrazole H-5), 10.21 (s, 1H, $\underline{NH}SO_2CH_3$, D_2O exchangeable); MS m/z (ES^+) 536.12 (M +) (100 %). Anal. Calcd. For $C_{26}H_{24}N_4O_5S_2$: C, 58.19; H, 4.51; N, 10.44; Found; C, 58.06; H, 4.38; N, 10.66.

4.1.2. General procedure for synthesis of the N-substituted acetamide derivatives (9a-f):

Chloro acetyl chloride (2.2 mmol) was added in a dropwise manner to an ice cooled solution of the appropriate chalcone derivatives (**8a-f,** 2.0 mmol), in dimethylformamide (20 ml) then the mixture was stirred at room temperature for 24 h, the resulting formed solid was filtered, dried and crystallized from ethanol to give the final *N*-substituted acetamide derivatives **(9a-f)**: Physical and spectral data are listed below:

4.1.2.1. (E)-2-chloro-N-(4-(3-(1-(4-(methylsulfonyl)phenyl)-3-phenyl-1H-pyrazol-4-yl)acryloyl)phenyl)acetamide (9a). Yield 81 %; yellowish brown solid; m.p. 222–224 °C; IR (KBr): 3413 (NH), 3120 (C═H aromatic), 2924 (C—H aliphatic), 1672 (ketonic C═O), 1595 (amidic C═O), 1533 (-C═C-), 1505 (C═N), 1403, 1144 (SO_2CH_3) cm^1; ^1H NMR (DMSO-d_6, 400 MHz, δ, ppm): 3.30 (s, 3H, $SO_2\underline{CH_3}$), 4.28 (s, 2H, CH_2), 7.49 (d, J = 8.0 Hz, 2H, acetamidophenyl H-2, H-6), 7.56 (m, 3H, phenyl H-3, H-4, H-5), 7.68 (d, J = 15.2 Hz, 1H, CH = C olifenic proton H_α), 7.80 (d, J = 15.2 Hz, 1H, CH = C olifenic proton H_β), 7.93 (d, J = 8.0 Hz, 2H, phenyl H-2, H-6), 8.11 (d, J = 8.0 Hz, 2H, acetamidophenyl H-3, H-5), 8.19 (d, J = 8.2 Hz, 2H, 4-methanesulfonylphenyl H-2, H-6), 8.27 (d, J = 8.2 Hz, 2H, 4-methanesulfonylphenyl H-3, H-5), 9.52 (s, 1H, pyrazole H-5), 10.74 (s, 1H, NH, D_2O exchangeable); MS m/z (ES^+) 443.13 (M +) (100 %). Anal. Calcd. For $C_{25}H_{21}N_3O_3S$: C, 67.70; H, 4.77; N, 9.47; Found; C, 67.96; H, 4.98; N, 9.69.

4.1.2.2. (E)-2-chloro-N-(4-(3-(3-(4-methoxyphenyl)-1-(4-(methylsulfonyl)phenyl)-1H-pyrazol-4-yl)acryloyl)phenyl)acetamide (9b). Yield 60 %; yellowish brown solid; m.p. 236–238 °C; IR (KBr): 3473 (NH), 3118 (C═H aromatic), 2929 (C—H aliphatic), 1658 (ketonic C═O), 1585 (amidic C═O), 1536 (-C═C-), 1403, 1176 (SO_2CH_3) cm^1; ^1H NMR (DMSO-d_6, 400 MHz, δ, ppm): 3.30 (s, 3H, $SO_2\underline{CH_3}$), 3.48 (s, 3H, OCH_3), 4.34 (s, 2H, CH_2), 7.08 (m, 4H, acetamidophenyl H-2, H-6 and 4-methoxyphenyl H-3, H-5), 7.14 (d, J = 15.2 Hz, 1H, CH = C olifenic proton H_α), 7.63 (d, J = 15.2 Hz, 1H, CH = C olifenic proton H_β), 7.91 (m, 4H, 4-methoxyphenyl H-2, H-6 and acetamidophenyl H-3, H-5), 8.12 (d, J = 8.2 Hz, 2H, 4-methanesulfonylphenyl H-2, H-6), 8.26 (d, J = 8.2 Hz, 2H, 4-methanesulfonylphenyl H-3, H-5), 9.52 (s, 1H, pyrazole H-5), 10.74 (s, 1H, NH, D_2O exchangeable); MS m/z (ES^+) 549.11 (M +) (100 %). Anal. Calcd. For $C_{28}H_{24}ClN_3O_5S$: C, 61.14; H, 4.40; N, 7.64; Found; C, 61.32; H, 4.27; N, 7.32.

4.1.2.3. (E)-2-chloro-N-(4-(3-(3-(4-chlorophenyl)-1-(4-(methylsulfonyl)phenyl)-1H-pyrazol-4-yl)acryloyl)phenyl)acetamide (9c). Yield 59 %; yellowish brown solid; m.p. 165–167 °C; IR (KBr): 3414 (NH), 3101 (C═H aromatic), 2924 (C—H aliphatic), 1651 (ketonic C═O), 1596 (amidic C═O), 1532 (-C═C-), 1504 (C═N), 1405, 1147 (SO_2CH_3) cm^1; ^1H NMR (DMSO-d_6, 400 MHz, δ, ppm): 3.31 (s, 3H, $SO_2\underline{CH_3}$), 4.33 (s, 2H, CH_2), 7.54 (d, J = 15.2 Hz, 1H, CH = C olifenic proton H_α), 7.63 (d, J = 8.0 Hz, 2H, acetamidophenyl H-2, H-6), 7.71 (d, J = 8.0 Hz, 2H, 4-chlorophenyl H-2, H-6), 7.80 (d, J = 8.0 Hz, 2H, acetamidophenyl H-3, H-5), 7.91 (d, J = 15.2 Hz, 1H, CH = C olifenic proton H_β), 8.09 (d, J = 8.0 Hz, 2H, 4-chlorophenyl H-3, H-5), 8.18 (d, J = 8.2 Hz, 2H, 4-methanesulfonylphenyl H-2, H-6), 8.26 (d, J = 8.2 Hz, 2H, 4-methanesulfonylphenyl H-3, H-5), 9.56 (s, 1H, pyrazole H-5), 10.73 (s, 1H, NH, D_2O exchangeable); MS m/z (ES^+) 553.06 (M +) (100 %). Anal. Calcd. For $C_{27}H_{21}Cl_2N_3O_4S$: C, 58.49; H, 3.82; N, 7.58; Found; C, 58.22; H, 4.06; N, 7.45.

4.1.2.4. (E)-2-chloro-N-(4-(3-(1-(4-(methylsulfonyl)phenyl)-3-(4-nitrophenyl)-1H-pyrazol-4-yl)acryloyl)phenyl)acetamide (9d). Yield 74 %; yellowish brown solid; m.p. 244–246 °C; IR (KBr): 3408 (NH), 3116 (C═H aromatic), 2926 (C—H aliphatic), 1685 (ketonic C═O), 1595 (amidic C═O), 1530 (-C═C-), 1504 (C═N), 1406, 1147 (SO_2CH_3) cm^1; ^1H NMR (DMSO-d_6, 400 MHz, δ, ppm): 3.30 (s, 3H, $SO_2\underline{CH_3}$), 4.31 (s, 2H, CH_2), 7.86 (d, J = 15.2 Hz, 1H, CH = C olifenic proton H_α), 7.95 (d, J = 8.0 Hz, 2H, acetamidophenyl H-2, H-6), 8.03 (d, J = 8.0 Hz, 2H, 4-nitrophenyl H-2, H-6), 8.14 (d, J = 8.0 Hz, 2H, acetamidophenyl H-3, H-5), 8.16 (d, J = 15.2 Hz, 1H, CH = C olifenic proton H_β), 8.25 (d, J = 8.0 Hz, 2H, 4-nitrophenyl H-3, H-5), 8.37 (d, J = 8.2 Hz, 2H, 4-methanesulfonylphenyl H-2, H-6), 8.41 (d, J = 8.2 Hz, 2H, 4-methanesulfonylphenyl H-3, H-5), 9.60 (s, 1H, pyrazole H-5), 10.60 (s, 1H, NH, D_2O exchangeable); MS m/z (ES^+) 564.09 (M +) (100 %). Anal. Calcd. For $C_{27}H_{21}ClN_4O_6S$: C, 57.40; H, 3.75; N, 9.92; Found; C, 57.72; H, 3.68; N, 9.74.

4.1.2.5. (E)-N-(4-(3-(3-(4-bromophenyl)-1-(4-(methylsulfonyl)phenyl)-1H-pyrazol-4-yl)acryloyl)phenyl)-2-chloroacetamide (9e). Yield 66 %; yellowish brown solid; m.p. 258–260 °C; IR (KBr): 3414 (NH), 3100 (C═H aromatic), 2925 (C—H aliphatic), 1651 (ketonic C═O), 1596 (amidic C═O), 1532 (-C═C-), 1504 (C═N), 1405, 1146 (SO_2CH_3) cm^1; ^1H NMR (DMSO-d_6, 400 MHz, δ, ppm): 3.31 (s, 3H, $SO_2\underline{CH_3}$), 4.32 (s, 2H, CH_2), 7.56 (d, J = 15.2 Hz, 1H, CH = C olifenic proton H_α), 7.64 (d, J = 8.0 Hz, 2H, acetamidophenyl H-2, H-6), 7.77 (d, J = 8.0 Hz, 2H, 4-bromophenyl H-2, H-6), 7.82 (d, J = 8.0 Hz, 2H, acetamidophenyl H-3, H-5), 7.88 (d, J = 15.2 Hz, 1H, CH = C olifenic proton H_β), 8.09 (d, J = 8.0 Hz, 2H, 4-bromophenyl H-3, H-5), 8.16 (d, J = 8.2 Hz, 2H, 4-methanesulfonylphenyl H-2, H-6), 8.21 (d, J = 8.2 Hz, 2H, 4-methanesulfonylphenyl H-3, H-5), 9.57 (s, 1H, pyrazole H-5), 10.74 (s, 1H, NH, D_2O exchangeable); MS m/z (ES^+) 597.01 (M +) (100 %). Anal. Calcd. For $C_{27}H_{21}BrClN_3O_4S$: C, 54.15; H, 3.53; N, 7.02; Found; C, 54.52; H, 3.88; N, 7.15.

4.1.2.6. (E)-2-chloro-N-(4-(3-(3-(4-(methylsulfonamido)phenyl)-1-(4-(methylsulfonyl)phenyl)-1H-pyrazol-4-yl)acryloyl)phenyl)acetamide (9f).

Yield 57 % yellow solid; m.p. 210–212 °C; IR (KBr): 3472 (NHSO$_2$CH$_3$), 3412 (CONH), 3116 (C═H aromatic), 2926 (C—H aliphatic), 1657 (ketonic C═O), 1594 (amidic C═O), 1529 (-C═C-), 1504 (C═N), 1403, 1144 (SO$_2$CH$_3$) cm^1; ^{1}H NMR (DMSO-d_6, 400 MHz, δ, ppm): 3.08 (s, 3H, NHSO$_2$CH$_3$), 3.29 (s, 3H, SO$_2$CH$_3$), 4.30 (s, 2H, NH$_2$, D$_2$O exchangeable); 7.41 (d, J = 8.0 Hz, 2H, acetamidophenyl H-3, H-5), 7. 65 (d, J = 15.2 Hz, 1H, CH = C olifenic proton H$_\alpha$), 7.67 (d, J = 8.0 Hz, 2H, *N*-phenylmethanesulfonamide H-3, H-5), 7.70 (d, J = 8.0 Hz, 2H, *N*-phenylmethanesulfonamide H-2, H-6), 7.80 (d, 2H, acetamidophenyl H-2, H-6), 7.90 (d, J = 15.2 Hz, 1H, CH = C olifenic proton H$_\beta$), 8.14 (d, J = 8.2 Hz, 2H, 4-methanesulfonylphenyl H-2, H-6), 8.21 (d, J = 8.2 Hz, 2H, 4-methanesulfonylphenyl H-3, H-5), 9.54 (s, 1H, pyrazole H-5), 10.05 (s, 1H, NHCO, D$_2$O exchangeable), 10.60 (s, 1H, NHSO$_2$CH$_3$, D$_2$O exchangeable); MS *m/z* (ES$^+$) 536.12 (M +) (100 %). Anal. Calcd. For C$_{26}$H$_{24}$N$_4$O$_5$S$_2$: C, 58.19; H, 4.51; N, 10.44; Found; C, 58.06; H, 4.38; N, 10.66.

4.1.3. General procedure for synthesis of the oxoethyl nitrate derivatives (10a-f):

A solution of the appropriate chloroacetamide (**9a-d**, 2.0 mmol) in dry acetonitrile (10 ml) (for compounds **9e,f** the reaction is carried out in mixture of DMF and acetonitrile in 1:1 ratio as solvent) was treated portion wise with a solution of silver nitrate (2.2 mmol) in dry acetonitrile (5 ml) and the whole mixture was heated under reflux for 8 h. The mixture was filtered, evaporated to dryness and the obtained residue was crystalized from methanol to give the final oxoethyl nitrate derivatives **(10a-f)**: Physical and spectral data are listed below:

4.1.3.1. ***(E and Z)-2-((4-(3-(1-(4-(methylsulfonyl)phenyl)-3-phenyl-1H-pyrazol-4-yl)acryloyl)phenyl)amino)-2-oxoethyl nitrate (10a)***. Yield 55 %; grey solid; m.p. 218–220 °C; IR (KBr): 3283 (NH), 3122 (C═H aromatic), 2924 (C—H aliphatic), 1672 (ketonic C═O), 1629 (amidic C═O), 1595 (N═O), 1534 (-C═C-), 1505 (C═N), 1401, 1141 (SO$_2$CH$_3$) cm^1; ^{1}H NMR (DMSO-d_6, 400 MHz, δ, ppm): 3.31 (s, 3.6H, two SO$_2$CH$_3$ of both *E* and *Z* isomers), 4.34, 5.14 (2 s, 2.2H, CH$_2$ of both *E* and *Z* isomers), 7.54 (m, 3.6H, phenyl H-3, H-4, H-5 of both *E* and *Z* isomers), 7.61 (d, J = 14.8 Hz, 1H, CH = C olifenic proton H$_\alpha$ of *E* isomer), 7.69 (d, J = 7.2 Hz, 2.2H, acetamidophenyl H-2, H-6 of both *E* and *Z* isomers),7.80 (d, J = 8.4 Hz, 0.2H, CH = C olifenic proton H$_\alpha$ of *Z* isomer), 7.89 (d, J = 14.8 Hz, 1H, CH = C olifenic proton H$_\beta$ of *E* isomer), 7.94 (d, J = 8.4 Hz, 2.4H, phenyl H-2, H-6 of both *E* and *Z* isomers), 8.05 d, J = 8.4 Hz, 0.2H, CH = C olifenic proton H$_\beta$ of *Z* isomer), 8.08 (d, J = 7.2 Hz, 2.4H, acetamidophenyl H-3, H-5 of both *E* and *Z* isomers), 8.14 (d, J = 8.8 Hz, 2.4H, 4-methanesulfonylphenyl H-2, H-6 of both *E* and *Z* isomers), 8.20 (d, J = 8.8 Hz, 2.4H, 4-methanesulfonylphenyl H-3, H-5 of both *E* and *Z* isomers), 9.29, 9.58 (2 s, 1.2H, pyrazole H-5 of both *E* and *Z* isomers), 10.19, 10.70 (2 s, 1.2H, NH, D$_2$O exchangeable of both *E* and *Z* isomers); ^{13}C NMR (DMSO-d_6) δ 44.06, 62.44, 88.50, 119.31, 120.19, 122.62, 128.94, 129.49, 129.94, 130.12, 131.99, 132.97, 133.44, 133.60, 139.10, 142.77, 143.45, 143.59, 154.23, 170.71, 187.65; MS *m/z* (ES$^+$) 546.12 (M +) (100 %). Anal. Calcd. For C$_{27}$H$_{22}$N$_4$O$_7$S: C, 59.33; H, 4.06; N, 10.25; Found; C, 59.15; H, 4.08; N, 9.96.

4.1.3.2. ***(E and Z)-2-((4-(3-(3-(4-methoxyphenyl)-1-(4-(methylsulfonyl)phenyl)-1H-pyrazol-4-yl)acryloyl)phenyl)amino)-2-oxoethyl nitrate (10b)***. Yield 62 %; grey solid; m.p. 221–223 °C; IR (KBr): 3445 (NH), 3118 (C═H aromatic), 2929 (C—H aliphatic), 1657 (ketonic C═O), 1596 (amidic C═O), 1595 (N═O), 1530 (-C═C-), 1505 (C═N), 1403, 1144 (SO$_2$CH$_3$) cm^1; ^{1}H NMR (DMSO-d_6, 400 MHz, δ, ppm): 3.31 (s, 3.6H, two SO$_2$CH$_3$ of both *E* and *Z* isomers), 3.86 (s, 3.6H, two OCH$_3$ of both *E* and *Z* isomers), 4.33, 5.14 (2 s, 2.2H, CH$_2$ of both *E* and *Z* isomers), 7.14 (d, J = 8.4 Hz, 2.4H, acetamidophenyl H-2, H-6 of both *E* and *Z* isomers), 7.63 (d, J = 8.4 Hz, 2.4H, 4-methoxyphenyl H-3, H-5 of both *E* and *Z* isomers), 7.68 (d, J = 16.0 Hz, 1H, CH = C olifenic proton H$_\alpha$ of *E* isomer), 7.87 (d, J = 8.4 Hz, 0.2H, CH = C olifenic proton H$_\alpha$ of *Z* isomer), 7.88 (d, J = 16.0 Hz, 1H, CH = C olifenic proton H$_\beta$ of *E* isomer), 7.94 (d, J = 8.4 Hz, 2.4H, 4-methoxyphenyl H-2, H-6 of both *E* and *Z* isomers), 8.08 (d, J = 8.4 Hz, 0.2H, CH = C olifenic proton H$_\beta$ of *Z* isomer), 8.10 (d, J = 8.4 Hz, 2.4H, acetamidophenyl H-3, H-5 of both *E* and *Z* isomers), 8.13 (d, J = 8.8 Hz, 2.4H, 4-methanesulfonylphenyl H-2, H-6 of both *E* and *Z* isomers), 8.19 (d, J = 8.8 Hz, 2.4H, 4-methanesulfonylphenyl H-3, H-5 of both *E* and *Z* isomers), 9.28, 9.55 (2 s, 1.2H, pyrazole H-5 of both *E* and *Z* isomers), 10.18, 10.70 (2 s, 1H, NH, D$_2$O exchangeable of both *E* and *Z* isomers); ^{13}C NMR (DMSO-d_6) δ 44.07, 55.78, 88.40, 114.90, 119.20, 119.52, 122.48, 124.30, 129.48, 130.27, 130.34, 130.62, 133.01, 133.59, 138.96, 142.80, 154.08, 157.63, 160.39, 160.43, 170.71, 187.64; MS *m/z* (ES$^+$) 576.13 (M +) (100 %). Anal. Calcd. For C$_{28}$H$_{24}$N$_4$O$_8$S: C, 58.33; H, 4.20; N, 9.72; Found; C, 58.68; H, 4.56; N, 9.90.

4.1.3.3. ***(E)-2-((4-(3-(3-(4-chlorophenyl)-1-(4-(methylsulfonyl)phenyl)-1H-pyrazol-4-yl)acryloyl)phenyl)amino)-2-oxoethyl nitrate (10c)***. Yield 52 %; grey solid; m.p. 263–265 °C; IR (KBr): 3452 (NH), 3122 (C═H aromatic), 2925 (C—H aliphatic), 1662 (ketonic C═O), 1598 (amidic C═O), 1595 (N═O), 1533 (-C═C-), 1503 (C═N), 1401, 1144 (SO$_2$CH$_3$) cm^1; ^{1}H NMR (DMSO-d_6, 400 MHz, δ, ppm): 3.37 (s, 3.0H, SO$_2$CH$_3$), 4.33, 5.28 (2 s, 2.0H, CH$_2$ of both conformational isomers), 7.61 (d, J = 15.6 Hz, 1H, CH = C olifenic proton H$_\alpha$), 7.63 (d, J = 7.6 Hz, 2.0H, acetamidophenyl H-2, H-6), 7.71 (d, J = 7.6 Hz, 2.0H, 4-chlorophenyl H-2, H-6), 7.79 (d, J = 8.0 Hz, 2.0H, acetamidophenyl H-3, H-5), 7.88 (d, J = 15.6 Hz, 1H, CH = C olifenic proton H$_\beta$), 8.09 (d, J = 8.8 Hz, 2.0H, 4-chlorophenyl H-3, H-5), 8.14 (d, J = 8.2 Hz, 2.4H, 4-methanesulfonylphenyl H-2, H-6), 8.19 (d, J = 8.2 Hz, 2.0H, 4-methanesulfonylphenyl H-3, H-5), 9.56 (s, 1.0H, pyrazole H-5 of both conformational isomers), 10.70, 10.81 (2 s, 1.0H, NH, D$_2$O exchangeable of both conformational isomers); ^{13}C NMR (DMSO-d_6) δ 44.05, 70.05, 119.35, 122.87, 129.46, 129.50, 129.91, 130.13, 130.21, 130.60, 130.82, 133.00, 133.21, 134.37, 139.16, 142.65, 143.31, 152.90, 164.92, 165.75, 187.58; MS *m/z* (ES$^+$) 580.08 (M +) (100 %). Anal. Calcd. For C$_{27}$H$_{21}$ClN$_4$O$_7$S: C, 55.82; H, 3.64; Cl, 6.10; N, 9.64; Found; C, 56.10; H, 3.88; N, 9.78.

4.1.3.4. ***(E)-2-((4-(3-(1-(4-(methylsulfonyl)phenyl)-3-(4-nitrophenyl)-1H-pyrazol-4-yl)acryloyl)phenyl)amino)-2-oxoethyl nitrate (10d)***. Yield 66 %; grey solid; m.p. 278–280 °C; IR (KBr): 3274 (NH), 3074 (C═H aromatic), 2927 (C—H aliphatic), 1656 (ketonic C═O), 1599 (amidic C═O), 1595 (N═O), 1528 (-C═C-), 1504 (C═N), 1344, 1146 (SO$_2$CH$_3$) cm^1; ^{1}H NMR (DMSO-d_6, 400 MHz, δ, ppm): 3.30 (s, 3H, SO$_2$CH$_3$), 5.29 (s, 2H, CH$_2$), 7.78 (d, J = 15.2 Hz, 1H, CH = C olifenic proton H$_\alpha$), 8.00 (d, J = 8.0 Hz, 2H, acetamidophenyl H-2, H-6), 8.14 (d, J = 8.0 Hz, 2H, 4-nitrophenyl H-2, H-6), 8.24 (d, J = 8.0 Hz, 2H, acetamidophenyl H-3, H-5), 8.26 (d, J = 15.2 Hz, 1H, CH = C olifenic proton H$_\beta$), 8.27 (d, J = 8.0 Hz, 2H, 4-nitrophenyl H-3, H-5), 8.37 (d, J = 8.2 Hz, 2H, 4-methanesulfonylphenyl H-2, H-6), 8.43 (d, J = 8.2 Hz, 2H, 4-methanesulfonylphenyl H-3, H-5), 9.61 (2 s, 1H, pyrazole H-5), 10.06 (s, 1H, NH, D$_2$O exchangeable); ^{13}C NMR (DMSO-d_6) δ 44.02, 70.07, 119.28, 119.40, 122.88, 129.55, 130.00, 130.14, 130.61, 130.93, 132.55, 133.21, 133.26, 134.38, 139.17, 142.66, 142.91, 143.32, 164.94, 166.16, 188.60; MS *m/z* (ES$^+$) 591.11 (M +) (100 %). Anal. Calcd. For C$_{27}$H$_{21}$N$_5$O$_9$S: C, 54.82; H, 3.58; N, 11.84; Found; C, 54.95; H, 3.44; N, 11.72.

4.1.3.5. ***(E)-2-((4-(3-(3-(4-bromophenyl)-1-(4-(methylsulfonyl)phenyl)-1H-pyrazol-4-yl)acryloyl)phenyl)amino)-2-oxoethyl nitrate (10e)***. Yield 66 %; grey solid; m.p. 292–294 °C; IR (KBr): 3421 (NH), 3110 (C═H aromatic), 2925 (C—H aliphatic), 1655 (ketonic C═O), 1598 (amidic C═O), 1595 (N═O), 1532 (-C═C-), 1503 (C═N), 1382, 1148 (SO$_2$CH$_3$) cm^1; ^{1}H NMR (DMSO-d_6, 400 MHz, δ, ppm): 3.30 (s, 3H, SO$_2$CH$_3$), 5.28 (s, 2H, CH$_2$), 7.61 (d, J = 15.2 Hz, 1H, CH = C olifenic proton H$_\alpha$), 7.65 (d, J = 8.0 Hz, 2H, acetamidophenyl H-2, H-6), 7.78 (d,

J = 8.0 Hz, 2H, 4-bromophenyl H-2, H-6), 7.89 (d, J = 15.2 Hz, 1H, CH = C olifenic proton H_β), 7.93 (d, J = 8.0 Hz, 2H, acetamidophenyl H-3, H-5), 8.08 (d, J = 8.0 Hz, 2H, 4-bromophenyl H-3, H-5), 8.13 (d, J = 8.2 Hz, 2H, 4-methanesulfonylphenyl H-2, H-6), 8.20 (d, J = 8.2 Hz, 2H, 4-methanesulfonylphenyl H-3, H-5), 9.59 (s, 1H, pyrazole H-5), 10.84 (s, 1H, NH, D_2O exchangeable); ^{13}C NMR (DMSO-d_6) δ 44.02, 70.07, 119.27, 119.39, 119.53, 123.05, 123.31, 129.50, 129.99, 130.35, 130.89, 131.21, 131.91, 132.47, 132.85, 133.03, 133.23, 139.23, 142.66, 152.97, 163.04; MS *m/z* (ES^+) 624.03 (M +) (100 %). Anal. Calcd. For $C_{27}H_{21}BrN_4O_7S$: C, 51.85; H, 3.38; N, 8.96; Found; C, 51.72; H, 3.16; N, 9.14.

4.1.3.6. *(E)-2-((4-(3-(3-(4-(methylsulfonamido)phenyl)-1-(4-(methylsulfonyl)phenyl)-1H-pyrazol-4-yl)acryloyl)phenyl)amino)-2-oxoethyl nitrate (10f)*.

Yield 62 % grey solid; m.p. 270–272 °C; IR (KBr): 3421 (NHSO$_2$CH$_3$), 3412 (CONH), 3110 (C═H aromatic), 2925 (C—H aliphatic), 1655 (ketonic C═O), 1599 (amidic C═O), 1595 (N═O), 1532 (-C═C-), 1504 (C═N), 1382, 1148 (SO_2CH_3) cm^1; ^{1}H NMR (DMSO-d_6, 400 MHz, δ, ppm): 2.74, 2.90 (2 s, 3H, NHSO$_2$CH$_3$), 3.31 (s, 3H, SO$_2$CH$_3$), 5.28 (s, 2H, CH_2, D_2O exchangeable), 7.63 (d, J = 15.2 Hz, 1H, CH = C olifenic proton H_α), 7.68 (d, J = 8.0 Hz, 2H, acetamidophenyl H-3, H-5), 7.80 (d, J = 8.0 Hz, 2H, *N*-phenylmethanesulfonamide H-3, H-5), 7.94 (d, J = 8.0 Hz, 2H, *N*-phenylmethanesulfonamide H-2, H-6), 8.08 (d, J = 15.2 Hz, 1H, CH = C olifenic proton H_β), 8.11 (d, 2H, acetamidophenyl H-2, H-6), 8.13 (d, J = 8.2 Hz, 2H, 4-methanesulfonylphenyl H-2, H-6), 8.20 (d, J = 8.2 Hz, 2H, 4-methanesulfonylphenyl H-3, H-5), 9.59 (2 s, 1H, pyrazole H-5), 10.82 (s, 1H, NHCO, D_2O exchangeable), 10.90, 11.04 (2 s, 1H, NHSO$_2$CH$_3$, D_2O exchangeable); ^{13}C NMR (DMSO-d_6) δ 44.04, 45.52 70.07, 119.18, 119.45, 122.88, 123.12, 129.41, 130.10, 130.25, 130.90, 132.48, 133.22, 133.26, 134.38, 139.27, 142.67, 142.67, 152.98, 153.69, 166.16, 188.64; MS *m/z* (ES^+) 536.12 (M +) (100 %). Anal. Calcd. For $C_{28}H_{25}N_5O_9S_2$: C, 52.58; H, 3.94; N, 10.95; Found; C, 52.24; H, 3.88; N, 10.86.

4.1.4. *General procedure for synthesis of the aldoxime derivatives (11a-f):*

A solution of the appropriate pyrazole aldehydes (**7a-f**, 2.0 mmol) in dry acetonitrile (10 ml) was treated portion wise with a solution of hydroxylamine hydrochloride (2.0 mmol) in dry acetonitrile (5 ml) in addition of catalytic amount of sodium acetate, the whole mixture was heated under reflux for 8 h. The formed precipitate was filtered, washed several time with water, dried and crystalized from ethanol to give the final aldoxime derivatives **(11a-f)**: Physical and spectral data are listed below:

4.1.4.1. *(syn and anti)-1-(4-(methylsulfonyl)phenyl)-3-phenyl-1H-pyrazole-4-carbaldehyde oxime (11a)*.

Yield 79 %; white solid; m.p. 178–180 °C; IR (KBr): 3248 (OH), 3115 (C═H aromatic), 1594 (C═N), 1539 (-C═C-), 1368, 1141 (SO_2CH_3) cm^1; ^{1}H NMR (DMSO-d_6, 400 MHz, δ, ppm): 3.28 (two singlets, 3.2H, SO$_2$CH$_3$, of syn and anti-geometrical aldoximes), 7.46 (s, 1H, anti-aldoxime proton), 7.49–7.58 (m, 3.2H, phenyl H-3, H-4, H-5 of both syn and anti-geometrical isomer), 7.69–7.74 (d, J = 8.0 Hz, 2.2H, phenyl H-2, H-6 of both syn and anti-geometrical isomer), 8.08 (d, J = 8.8 Hz, 2.2H, 4-methanesulfonylphenyl H-2, H-6 of both syn and anti-aldoximes), 8.14 (s, 0.2H, aldoxime proton of *syn*-geometrical isomer), 8.24 (d, J = 8.8 Hz, 0.4H, 4-methanesulfonylphenyl H-3, H-5 of syn aldoxime), 8.26 (d, J = 8.8 Hz, 2.0H, 4-methanesulfonylphenyl H-3, H-5 of anti-aldoxime), 9.02 (s, 0.2H, pyrazole H-5 of syn aldoxime), 9.33 (s, 1.0H, pyrazole H-5 of anti-aldoxime), 11.20 (s, 0.2H, *syn*-aldoxime OH, D_2O exchangeable), 11.94 (s, 1.0H, anti-aldoxime OH, D_2O exchangeable); ^{13}C NMR (DMSO-d_6) δ 44.06, 112.62, 119.36, 119.73, 128.67, 131.82, 132.38, 137.03, 138.83, 140.93, 141.18, 142.89, 153.48; MS *m/z* (ES^+) 341.08 (M +) (100 %). Anal. Calcd. For $C_{17}H_{15}N_3O_3S$: C, 59.81; H, 4.43; N, 12.31; Found; C, 59.66; H, 4.16; N, 12.12.

4.1.4.2. *(syn and anti)-3-(4-methoxyphenyl)-1-(4-(methylsulfonyl) phenyl)-1H-pyrazole-4-carbaldehyde oxime (11b)*.

Yield 81 %; white solid; m.p. 184–186 °C; IR (KBr): 3419 (OH), 3070 (C═H aromatic), 1595 (C═N), 1512 (-C═C-), 1355, 1141 (SO_2CH_3) cm^1; ^{1}H NMR (DMSO-d_6, 400 MHz, δ, ppm): 3.44 (two singlets, 4.5H, two SO$_2$CH$_3$ of both syn and anti-aldoximes), 3.79 (two singlets, 4.5H, two OCH_3 of both syn and anti-aldoximes), 7.04 (d, J = 8.2 Hz, 1.0H, 4-methoxyphenyl H-3, H-5 of *syn*-aldoxime), 7.08 (d, J = 8.2 Hz, 2.0H, 4-methoxyphenyl H-3, H-5 of anti-aldoxime), 7.45 (s, 1H, anti-aldoxime proton), 7.58 (d, J = 8.2 Hz, 2.0H, 4-methoxyphenyl H-2, H-6 of anti-aldoxime), 7.65 (d, J = 8.2 Hz, 1.0H, 4-methoxyphenyl H-2, H-6 of *syn*-aldoxime), 8.05 (d, J = 8.2 Hz, 2.2H, 4-methanesulfonylphenyl H-2, H-6 of both syn and anti-aldoximes), 8.14 (s, 0.2H, *syn*-aldoxime proton), 8.22 (d, J = 8.2 Hz, 1.0H, 4-methanesulfonylphenyl H-3, H-5 of *syn*-aldoxime), 8.24 (d, J = 8.2 Hz, 2H, 4-methanesulfonylphenyl H-3, H-5 of anti-aldoxime), 8.98 (s, 0.5H, pyrazole H-5 of *syn*-aldoxime), 9.30 (s, 1.0H, pyrazole H-5 of anti-aldoxime), 11.11 (s, 0.5H, *syn*-aldoxime OH, D_2O exchangeable), 11.91 (s, 1.0H, anti-aldoxime OH, D_2O exchangeable); ^{13}C NMR (DMSO-d_6) δ 44.05, 55.60, 112.44, 114.53, 119.23, 119.59, 124.08, 130.45, 132.21, 137.24, 141.14, 142.90, 153.35, 160.24; MS *m/z* (ES^+) 371.09 (M +) (100 %). Anal. Calcd. For $C_{18}H_{17}N_3O_4S$: C, 58.21; H, 4.61; N, 11.31; Found; C, 58.04; H, 4.44; N, 11.26.

4.1.4.3. *(syn and anti)-3-(4-chlorophenyl)-1-(4-(methylsulfonyl)phenyl)-1H-pyrazole-4-carbaldehyde oxime (11c)*.

Yield 78 %; white solid; m.p. 212–214 °C; IR (KBr): 3240 (OH), 3048 (C═H aromatic), 1596 (C═N), 1541 (-C═C-), 1365, 1143 (SO_2CH_3) cm^1; ^{1}H NMR (DMSO-d_6, 400 MHz, δ, ppm): 3.37 (two singlets, 3.8H, SO$_2$CH$_3$ of both syn and anti-aldoxime), 7.43 (s, 1.0H, anti-aldoxime proton), 7.58 (d, J = 8.2 Hz, 0.4H, 4-chlorophenyl H-3, H-5 of *syn*-aldoxime), 7.58 (d, J = 8.2 Hz, 2.4H, 4-chlorophenyl H-3, H-5 of both syn and anti aldoximes), 7.71 (d, J = 8.2 Hz, 0.4H, 4-chlorophenyl H-2, H-6 of anti-aldoxime), 7.73 (d, J = 8.2 Hz, 0.4H, 4-chlorophenyl H-2, H-6 of *syn*-aldoxime), 8.09 (d, J = 8.2 Hz, 2.4H, 4-methanesulfonylphenyl H-2, H-6 of both syn and anti-aldoximes), 8.08 (s, 1/4H, *syn*-aldoxime proton), 8.24 (d, J = 8.2 Hz, 2H, 4-methanesulfonylphenyl H-3, H-5), 9.01 (s, 1/4H, pyrazole H-5 of *syn*-aldoxime), 9.32 (s, 1.0H, pyrazole H-5 of anti-aldoxime), 11.24 (s, 0.2H, *syn*-aldoxime OH, D_2O exchangeable), 11.98 (s, 1.0H, anti-aldoxime OH, D_2O exchangeable); ^{13}C NMR (DMSO-d_6) δ 44.07, 112.70, 119.74, 129.32, 130.41, 130.79, 130.84, 132.54, 134.22, 136.78, 139.01, 142.81, 152.12; MS *m/z* (ES^+) 375.04 (M +) (100 %). Anal. Calcd. For $C_{17}H_{14}ClN_3O_3S$: C, 54.33; H, 3.75; N, 11.18; Found; C, 54.14; H, 3.54; N, 11.44.

4.1.4.3.1. *(syn)-3-(4-chlorophenyl)-1-(4-(methylsulfonyl)phenyl)-1H-pyrazole-4-carbaldehyde oxime (11c):*.

^{1}H NMR (DMSO-d_6, 400 MHz, δ, ppm): 3.37 (singlets, 3H, SO$_2$CH$_3$), 7.24 (d 2H, 4-chlorophenyl H-3, H-5 of anti aldoxime), 7.26 (d 2H, 4-chlorophenyl H-2, H-6 of anti aldoxime), 7.36 (d, 2.0H, 4-methanesulfonylphenyl H-2, H-6 of anti-aldoxime), 7.39 (d, 2H, 4-methanesulfonylphenyl H-3, H-5), 7.41 (s, 1H, anti-aldoxime proton), 9.65 (s, 1.0H, pyrazole H-5 of anti-aldoxime), (s, 1.0H, anti-aldoxime OH) not detected.

4.1.4.4. *(E)-1-(4-(methylsulfonyl)phenyl)-3-(4-nitrophenyl)-1H-pyrazole-4-carbaldehyde oxime (11d)*.

Yield 88 %; white solid; m.p. 229–231 °C; IR (KBr): 3428 (OH), 3010 (C═H aromatic), 1595 (C═N), 1535 (-C═C-), 1342, 1147 (SO_2CH_3) cm^1; ^{1}H NMR (DMSO-d_6, 400 MHz, δ, ppm): 3.35 (s, 3H, SO$_2$CH$_3$), 7.56 (s, 1H, aldoxime proton), 8.02 (d, J = 8.0 Hz, 2H, 4-nitrophenyl H-3, H-5), 8.09 (d, J = 8.0 Hz, 2H, 4-nitrophenyl H-2, H-6), 8.29 (d, J = 8.0 Hz, 2H, 4-methanesulfonylphenyl H-2, H-6), 8.39 (d, J = 8.0 Hz, 2H, 4-methanesulfonylphenyl H-3, H-5), 9.39 (s, 1H, pyrazole H-5), 12.07 (s, 1H, aldoxime OH, D_2O exchangeable); ^{13}C NMR (DMSO-d_6) δ 44.04, 113.12, 119.99, 124.54, 129.35, 130.26, 132.94, 136.50, 138.41, 139.37, 142.70, 147.94, 151.05; MS *m/z* (ES^+) 386.07 (M +) (100 %). Anal. Calcd. For $C_{17}H_{14}N_4O_5S$: C, 52.84; H, 3.65; N,

14.50; Found; C, 52.64; H, 3.74; N, 14.28.

4.1.4.5. (E)-3-(4-bromophenyl)-1-(4-(methylsulfonyl)phenyl)-1H-pyrazole-4-carbaldehyde oxime (11e). Yield 85 %; white solid; m.p. 255–257 °C; IR (KBr): 3436 (OH), 3045 (C═H aromatic), 1594 (C═N), 1541 (-C═C-), 1364, 1142 (SO_2CH_3) cm^1; ^1H NMR (DMSO-d_6, 400 MHz, δ, ppm): 3.29 (s, 3H, $SO_2\underline{CH_3}$), 7.47 (s, 1H, aldoxime proton), 7.64 (d, J = 8.2 Hz, 2H, 4-bromophenyl H-3, H-5), 7.74 (d, J = 8.2 Hz, 2H, 4-bromophenyl H-2, H-6), 8.06 (d, J = 8.2 Hz, 2H, 4-methanesulfonylphenyl H-2, H-6), 8.23 (d, J = 8.2 Hz, 2H, 4-methanesulfonylphenyl H-3, H-5), 9.32 (s, 1H, pyrazole H-5), 12.00 (s, 1H, aldoxime OH, D_2O exchangeable); ^{13}C NMR (DMSO-d_6) δ 44.06, 112.67, 119.74, 122.89, 129.32, 131.08, 131.11, 132.32, 132.56, 136.77, 138.98, 142.79, 152.15; MS m/z (ES^+) 386.07 (M +) (100 %). Anal. Calcd. For $C_{17}H_{14}BrN_3O_3S$: C, 48.58; H, 3.36; N, 10.00; Found; C, 48.32; H, 3.10; N, 10.12.

(E)-*N*-(4-(4-((hydroxyimino)methyl)-1-(4-(methylsulfonyl)phenyl)-1*H*-pyrazol-3-yl)phenyl)methanesulfonamide *(11f):* Yield 85 %; white solid; m.p. 278–280 °C; IR (KBr): 3362 (OH), 3244 ($NHSO_2CH_3$), 3019 (C═H aromatic), 2932 (C═H aliphatic), 1534 (C═N), 1503 (-C═C-), 1371, 1149 (SO_2CH_3) cm^1; ^1H NMR (DMSO-d_6, 400 MHz, δ, ppm): 3.29 (s, 3H, $SO_2\underline{CH_3}$), 3.59 (s, 3H, $NHSO_2\underline{CH_3}$), 7.66 (d, J = 8.2 Hz, 2H, acetamidophenyl H-3, H-5), 7.86 (d, J = 8.2 Hz, 2H, acetamidophenyl H-2, H-6), 8.08 (d, J = 8.2 Hz, 2H, 4-methanesulfonylphenyl H-2, H-6), 8.25 (s, 1H, aldox ime proton), 8.27 (d, J = 8.2 Hz, 2H, 4-methanesulfonylphenyl H-3, H-5), 9.06, 9.36 (2 s, 1H, pyrazole H-5), 11.28, 12.01 (s, 1H, aldoxime OH, D_2O exchangeable), (s, 1H, $\underline{NH}CO$, D_2O exchangeable); ^{13}C NMR (DMSO-d_6) δ 43.52, 44.04, 116.47, 119.44, 119.89, 129.35, 129.75, 131.72, 131.96, 134.10, 138.95, 141.00, 142.77, 150.89; MS m/z (ES^+) 434.07 (M +) (100 %). Anal. Calcd. For $C_{18}H_{18}N_4O_5S_2$: C, 49.76; H, 4.18; N, 12.89; Found; C, 49.54; H, 4.42; N, 12.70.

4.2. Biological evaluation

4.2.1. In-vitro anti-inflammatory activity

The *in vitro* COX-1/COX-2 inhibition was determined using COX-1 Inhibitor Screening Kit-K548 (Biovision, S. Milpitas Blvd., Milpitas, CA 95035 USA) and COX-2 Inhibitor Screening Kit-K547 (Biovision, S. Milpitas Blvd., Milpitas, CA 95035 USA). The IC_{50} of testing compounds was determined. Also, the COX-2 selectivity indexes (S.I values) which are defined as IC_{50} (COX-1)/IC_{50} (COX-2) were calculated and compared with that of the standard drugs celecoxib (as a selective COX-2 inhibitor) according to the following procedure: **COX-1 inhibitor Screening Protocol:** Dissolve tested compounds in DMSO. Dilute to 10X the desired test concentration with COX Assay Buffer before use. Add 10 µl diluted test inhibitor or Assay Buffer into assigned wells as sample screen [S] or Enzyme Control [EC] (no inhibitor) respectively. Add 2 µl of SC560 and 8 µl COX Assay Buffer into one of the wells as Inhibitor Control [IC]. Dilute COX Cofactor 200 times by adding 2 µl of COX Cofactor to 398 µl of COX Assay Buffer just before use. Mix well. Prepare Arachidonic Acid solution by adding 5 µl of supplied Arachidonic Acid to 5 µl of NaOH just before use. Vortex briefly to mix. Dilute Arachidonic Acid/NaOH solution 10 times by adding 90 µl ddH_2O, vortex briefly to mix. Make as much as needed. Add 80 µl of Reaction Mix into each well. Use a multi-channel pipette to add 10 µl of diluted Arachidonic Acid/NaOH solution into each well to initiate all the reactions at the same time. Measure fluorescence (Ex/Em = 535/587 nm) kinetically at 25 °C for 5–10 min. **COX-2 inhibitor Screening Protocol:** Dissolve tested compounds in DMSO. Dilute to 10X the desired test concentration with COX Assay Buffer before use. Add 10 µl diluted test inhibitor or Assay Buffer into assigned wells as sample screen [S] or Enzyme Control [EC] (no inhibitor) respectively. Add 2 µl of Celecoxib and 8 µl COX Assay Buffer into one of the wells as Inhibitor Control [IC]. Dilute COX Cofactor 200 times by adding 2 µl of COX Cofactor to 398 µl of COX Assay Buffer just before use. Mix well. Prepare Arachidonic Acid solution by adding 5 µl of supplied Arachidonic Acid to 5 µl of NaOH just before use. Vortex briefly to mix. Dilute Arachidonic Acid/NaOH solution 10 times by adding 90 µl ddH_2O, vortex briefly to mix. Make as much as needed. Add 80 µl of Reaction Mix into each well. Use a multi-channel pipette to add 10 µl of diluted Arachidonic Acid/NaOH solution into each well to initiate the reactions at the same time. Measure fluorescence (Ex/Em = 535/587 nm) kinetically at 25 °C for 5–10 min.

4.2.2. Preliminary in-vitro anticancer screening

The anticancer activity of the synthesized compounds was screened using 60 different human tumor cell lines [67–69]. The human tumor cell lines were grown in RPMI 1640 medium containing 2 mM L-glutamine and 5 % fetal bovine. Cells were inoculated into 96 well microtiter plates into 100 µl at optical density ranging from 5000 to 40,000 cells/well depending on the doubling time of individual cell lines. Incubate the microtiter plates at 37 °C, 5 % CO_2, 95 % air and 100 % relative humidity for 24 h. then fix two plates of each cell line *in situ* using trichloroacetic acid (TCA) to characterize a measurement of cell population at the time of adding drug. Dissolve the prepared compounds in dimethyl sulfoxide (DMSO) at 400-folds the desired final maximum concentration and store frozen prior to use. Melt the frozen concentrate at time of drug addition, then dilute to twice the final concentration with complete medium containing 50 µg/mL gentamycin. Add the prepared compounds (100 µl) to the appropriate microtiter wells (100 µl) to yield the final compound concentration. incubate the plates at 37 °C, 5 % CO_2, 95 % air and 100 % relative humidity for 48 h. To fix the cells 50 µl of cold 50 % (w/v) TCA was gently added and the plates were incubated for 60 min at 4 °C. discard the supernatant, and wash the plates 5 times with tap water and dry in air. Sulphorhodamine B (SRB) solution (100 µl) at 0.4 % (w/v) in 1 % acetic acid was used as protein dye and added to each well then plates were incubated for 10 min at room temperature. Washing five times with 1 % acetic acid to remove unbound dye and plates were air dried. The bound stain was dissolved in 10 mµ trizma base and the absorbance was read at 515 nm wavelength using an automated plate reader. The treated cells percentage growth was calculated compared to the untreated control cells.

4.2.3. MTT assay for viability of cell

MTT colorimetric assay using Doxorubicin as standard was used for determination of the IC_{50} against breast, ovarian and melanoma cell lines (MCF-7, IGROV1 and SK-MEL-5), in addition to normal fibroblasts F180 (to show the effect of the synthesized compounds and doxorubicin on the normal cells) [70]. Where MCF-7, IGROV1, SK-MEL-5 and F180 cells were allowed to grow in 100 µl Dulbecco's Modified Eagle's Medium **DMEM** media in 96-well cell culture plate, supplemented with 1 % penicillin/streptomycin and were incubated at 37 °C until the concentration of the cells in the media was 5×10^4 cells/mL. The selected compounds and standards were dissolved in DMEM media at 1 mg/mL concentration. 10 fold serial dilutions were carried out to get the final concentrations (0.01–100 µM) and were incubated for 24 h. 50 µl/well of MTT 3-(4,5-dimethylthiazol-2-yl)-2,5-diphenyltetrazolium bromide was solubilized in phosphate buffered saline and incubate the cultures at 37 °C for 4 h with 5 % CO_2. 100 µl of isopropanol and 0.04 N HCl were added to all wells and mixed to dissolve the obtained crystals. Robonik P2000 spectrophotometer was used to read the absorbance at a wavelength of 490 nm.

4.2.4. Cell cycle analysis

Using flow cytometry, allow us to study the effect of compound **11a** on cell growth. [71] Compound **11a** was added on breast MCF-7 cells with (IC_{50} = 3.12 µM) for 24 h. rinsed breast cells with phosphate buffer saline (PBS), centrifuge, add 70 % ethanol, then, wash cells washed again with PBS and suspended with 0.1 mg/mL RNase. In addition, mark cells with 40 mg/mL propidium iodide (PI) and FACSCalibur flow cytometer (Becton Dickinson) was used to determine cell cycle

distribution. Moreover, the cell cycle distribution was calculated using Cell Quest software (Becton Dickinson) (Table 3).

4.2.5. Determination of apoptosis using Annexin-V

The apoptosis of compound **11a** was determined using Annexin-V-FITC method. [72] MCF-7 breast cells were treated with compound **11a** at its $IC_{50} = 3.12$ μM, then incubate cells for 24 h., collect the cells, rinse twice with PBS, and mark with mixture of fluorescein isothiocyanate (FITC), Annexin-V- and PI (propidium iodide) are left for 30 min at room temperature in the dark. FACSCalibur flow cytometer (BD Biosciences, San Jose, CA, USA) was used for analysis (Table 4). (SeeTable 5).

4.2.6. Aromatase inhibitory activity

Aromatase (CYP19A) inhibitor screening Kit-K984 (Biovision, S. Milpitas Blvd., Milpitas, CA 95035 USA) was used to determine the aromatase inhibitory activity and IC_{50} of compounds **10c, 11a and 11e** were determined in MCF-7 cells according to the following procedure: Dissolve test compounds into proper solvent to produce stock solutions. For each test compound, prepare a 5X solution of each desired test concentration by diluting in Aromatase Assay Buffer. Prepare the Recombinant Human Aromatase stock (2X) by reconstituting with 1 ml of Aromatase Assay Buffer. Mix contents thoroughly by vortexing to obtain a homogeneous solution and transfer the solution to a 15 ml conical tube. Bring the volume up to 2450 μl with Aromatase Assay Buffer and add 50 μl of the NADPH Generating System (100X) for a final total volume of 2.5 ml. Prepare reaction wells containing test compounds and corresponding no inhibitor controls (which may also serve as a solvent control), as well as a background control (containing no fluorogenic Aromatase Substrate) and (if desired) a positive inhibition control using 5 μM letrozole (5X solution, 1 μM final concentration). Incubate the plate for at least 10 min at 37 °C to allow test ligands to interact with aromatase. Start the reaction by adding 30 μl of the Aromatase Substrate/$NADP^+$ (3X) mixture to each well (aside from the background control) using a multichannel pipette, yielding a final reaction volume of 100 μl/well. Immediately (within 1 min) measure the fluorescence at Ex/Em = 488/527 nm in kinetic mode for 60 min.

4.3. Nitric oxide release measurement:

A solution of the appropriate compound **10a-f** and **11a-f** (20 μl) in DMSO was added to 2 ml of 1:1 v/v mixture of 50 mM phosphate buffer (pH 7.4) with methanol containing 5x10-4 M of *N*-acetyl-cysteine. The final concentration of drug was 10–4 M. the tested solutions were kept in an incubator for 1 h at 37 °C, 1 ml of the reaction mixture was treated with 250 μl of Griess reagent [sulfanilamide (2 g), *N*-naphthylethylenediamine dihydrochloride (0.2 g), 85 % phosphoric acid (10 ml) in distilled water (final volume: 100 ml)]. After 10 min at room temperature, the absorbance was measured at λ^{max} 540 nm. Sodium nitrite standard solutions (10–80 nmol/mL) were used to construct the calibration curve. The same procedure was repeated using different solutions of the target compounds 8a-f and 9a-f under the same conditions using 0.1 N HCl of pH 1 instead of phosphate buffer of pH 7.4 The results were expressed as the percentage of NO released relative to a theoretical maximum release of 1 mol NO/mol of test compound [73].

Table 4
Cell cycle analysis of compound **11a,** doxorubicin and control for breast MCF-7 cells.

Cell cycle phase	%G0-G1	%S	%G2-M	%Pre G1
9a	31.54	23.78	44.68	26.17
Doxorubicin	37.61	31.46	30.93	14.52
Control	57.05	31.82	11.13	2.18

Table 5
Apoptosis of compound **11a,** doxorubicin and control against breast MCF-7 cells.

	Total	Early	Late	Necrosis
9a	26.17	9.41	14.18	2.58
Doxorubicin	14.52	6.51	6.18	1.83
Control	2.18	0.92	0.23	1.03

4.4. Molecular modeling study

4.4.0.1. Molecular docking

The docking studies were operated using the OpenEye Modeling software [Fast Rigid Exhaustive Docking (FRED) Receptor, version 2.2.5; OpenEye Scientific Software, SantaFe, NM (USA); http://www.eyesopen.com], academic license (The Laboratory of Yaseen A. M. Mohamed Elshaier). A virtual library of target compounds was built, and their energies were minimized using the MMFF94 force field, followed by the generation of multi-conformers using the OMEGA application. The library was compiled in one file by Omega. The target proteins were retrieved from PDB and the created receptor was operated by OeDocking application. Both the ligand input file and the receptor input file were subjected to FRED to implement the molecular docking study. Multiple scoring functions were engaged to predict energy profile of the ligand-receptor complex. The vida application was used as a visualization method to represent the ligands pose and the potential binding interactions of the ligands to the receptor of interest.

4.4.0.2. Shape similarity and ROCS analysis

The basic method to represent shape and colour features in ROCS is using ROCS application Open Eye scientific software. The query molecules were selected based on high similarity [https://www.eyesopen.

Table 3
Physicochemical properties and color atoms representation for compounds using ROCS technique.

	Physicochemical properties					color atoms				
compound	**Mwt**	**LogP**	**PSA**	**Rotatable bond**	**No of heavy atom**	**donor**	**acceptor**	**No of rings**	**Anion**	**Hydrophobe**
MS4 (Co-crystallized ligand)	389	1.90	123	5	26	1	5	3	–	–
Celecoxib	381	3.47	77	4	56	–	3	3	–	–
10a	546	3.8	153	11	39	1	7	4	–	–
10b	625	4.6	153	11	40	1	7	4	–	1
10c	580	4.42	153	11	40	1	7	4	–	–
10d	591	3.72	199	12	42	1	9	4	–	–
10e	639	2.76	199	13	44	1	9	4	1	–
10f	576	3.66	162	12	41	1	8	4	–	–
11a	341	3.44	84	4	24	–	4	3	1	
11b	420	4.24	84	4	25	–	4	3	1	1
11c	375	4.06	84	4	25	–	4	3	1	–
11d	386	3.63	130	5	27	–	6	3	1	–
11e	434	2.45	130	6	29	–	6	3	2	–
11f	371	3.3	93	5	26	–	5	3	1	–

com/] Compounds library was adopted as the database file. Both query and database files were energy minimized by Omega applications. Personal PC in very fast using vROCS interface employed ROCS runs. vROCS was employed to run and analyze/visualize the results. ROCS application searched the database with the query to find molecules with similar shapes and colours. The result was visualized by Vida application.

Declaration of Competing Interest

The authors declare that they have no known competing financial interests or personal relationships that could have appeared to influence the work reported in this paper.

Data availability

Data will be made available on request.

Acknowledgments:

Prof. Dr. Wael A. A. Fadaly, Pharmaceutical Organic Chemistry Department, Faculty of Pharmacy, Beni-Suef University would like to acknowledge Research Institute of Medicinal & Aromatic plants, Beni-Suef University for providing the analysis work on Biotage Isolera One Flash Chromatograph.

Prof. Dr. Yaseen A. M. M. Elshaier, Organic & Medicinal Chemistry Department, Faculty of Pharmacy, University of Sadat City (USC), would like to acknowledge OpenEye scientific software for providing the academic license.

Appendix A. Supplementary material

Supplementary data to this article can be found online at https://doi.org/10.1016/j.bioorg.2023.106428.

References

[1] I. Ahmad, Shagufta, Recent developments in steroidal and nonsteroidal aromatase inhibitors for the chemoprevention of estrogen-dependent breast cancer, Eur. J. Med. Chem. 102 (2015) 375–386.
[2] M.R. Yadav, M.A. Barmade, R.S. Tamboli, P.R. Murumkar, Developing steroidal aromatase inhibitors-an effective armament to win the battle against breast cancer, Eur. J. Med. Chem. 105 (2015) 1–38.
[3] N. Adhikari, S.A. Amin, A. Saha, T. Jha, Combating breast cancer with non-steroidal aromatase inhibitors (NSAIs): understanding the chemico-biological interactions through comparative SAR/QSAR study, Eur. J. Med. Chem. 137 (2017) 365–438.
[4] Adhikari, Nilanjan; Amin, Sk. Abdul; Saha, Achintya; Jha, Tarun , Combating breast cancer with non-steroidal aromatase inhibitors (NSAIs): Understanding the chemico-biological interactions through comparative SAR/QSAR study. Eur. J. Med. Chem. 137: 365–438. Doi:10.1016/j.ejmech.2017.05.041.
[5] A. Irshad; Shagufta, Recent developments in steroidal and nonsteroidal aromatase inhibitors for the chemoprevention of estrogen-dependent breast cancer. Eur. J. Med. Chem. 102: 375–386. doi:10.1016/j.ejmech.2015.08.010.
[6] S. Zafer; E. Merve; B. Barkın; B. Sevde Nur; Y. Leyla; D. Seref Studies on non-steroidal inhibitors of aromatase enzyme; 4-(aryl/heteroaryl)-2-(pyrimidin-2-yl) thiazole derivatives. Bioorg. Med. Chem. 26 (8): 1986–1995. doi:10.1016/j.bmc.2018.02.048.
[7] N. Barbara, A. Barbara, L. Roberta, M. Antonio, S. Andrea, C. Mariantonia, G. Rossell, Identification of novel COX-2 / CYP19A1 axis involved in the mesothelioma pathogenesis opens new therapeutic opportunities, J. Experimental & Clin. Cancer Res. 40 (1) (2021) 257, https://doi.org/10.1186/s13046-021-02050-1.
[8] Edgar S. Díaz-Cruz, Charles L. Shapiro, and Robert W. Cyclooxygenase Inhibitors Suppress Aromatase Expression and Activity in Breast Cancer Cells. The Journal of Clinical Endocrinology & Metabolism (2005), 90 (5): 2563–2570. DOI: 10.1210/jc.2004-2029.
[9] R.W. Brueggemeier, E.S. Diaz-Cruz, Relationship between aromatase and cyclooxygenases in breast cancer: potential for new therapeutic approaches Minerva endocrinologica 31 (1) (2006) 13–26.
[10] C.P. de Souza, B. Alves, J. Waisberg, F. Fonseca, A. de Oliveira Carmo, F. Gehrke, Detection of COX-2 in liquid biopsy in patients with breast cancer, J. Clin. Pathol. 73 (2020) 826–829, https://doi.org/10.1136/jclinpath-2020-206576.
[11] K. Strasser-Weippl, M.J. Higgins, J.W. Chapman, J.N. Ingle, G.W. Sledge, G. T. Budd, M.J. Ellis, K.I. Pritchard, M.J. Clemons, T. Badovinac-Crnjevic, L. Han, K. A. Gelmon, M. Rabaglio, C. Elliott, L.E. Shepherd, P.E. Goss, Effects of celecoxib and low-dose aspirin on outcomes in adjuvant aromatase inhibitor-treated patients: CCTG, J. National Cancer Institute 110 (9) (2018) 1003–1008, https://doi.org/10.1093/jnci/djy017.
[12] A.L. Pedersen, J.L. Brownrout, C.J. Saldanha, Central administration of indomethacin mitigates the injury-induced upregulation of aromatase expression and estradiol content in the zebra finch brain, Endocrinology 158 (8) (2017) 2585–2592, https://doi.org/10.1210/en.2017-00346.
[13] R.E. Harris, K.K. Namboodiri, W.B. Farrar, Nonsteroidal anti- inflammatory drugs and breast cancer risk, Epidemiology 7 (1996) 203–205.
[14] G.R. Mayer, D. Marina, A.J. Paulo, d.N.R. Nascimento, F. Marcelo, C. Tuany, G.A. P. Vargas, V.T. Cunha, C.G. Dantas, S. Nauana,, COX-2 promotes mammary adipose tissue inflammation, local estrogen biosynthesis, and carcinogenesis in high-sugar/fat diet treated mice, Cancer lett. 502 (2021) 44–57, https://doi.org/10.1016/j.canlet.2021.01.003.
[15] R.E. Harris, F.M. Robertson, R.W. Brueggemeier, Genetic induction and upregulation of cyclooxygenase (COX) and aromatase (CYP19): an extension of the dietary fat hypothesis of breast cancer, Med. Hypotheses 52 (1999) 291–292, https://doi.org/10.1054/mehy.1998.0009.
[16] C.A. Velazquez, P.N. Praveen Rao, M.L. Citro, L.K. Keefer, E.E. Knaus, O2-acetoxymethyl-protected diazeniumdiolate-based NSAIDs (NONO-NSAIDs): synthesis, nitric oxide release, and biological evaluation studies, Bioorg. Med. Chem. 15 (14) (2007) 4767–4774, https://doi.org/10.1016/j.bmc.2007.05.009.
[17] S.V. Bhandari, J.K. Parikh, K.G. Bothara, T.S. Chitre, D.K. Lokwani, T.L. Devale, N. S. Modhave, V.S. Pawar, S. Panda, Design, synthesis, and evaluation of anti-inflammatory, analgesic, ulcerogenicity, and nitric oxide releasing studies of novel indomethacin analogs as non-ulcerogenic derivatives, J. Enzyme Inhib. Med. Chem. 25 (4) (2010) 520–530, https://doi.org/10.3109/14756360903357585.
[18] J.L. Wallace, M.J. Miller, Nitric oxide in mucosal defense: a little goes a long way, Gastroenterology 119 (2) (2000) 512–520, https://doi.org/10.1053/gast.2000.9304.
[19] K. Takeuchi, T. Yasuhiro, Y. Asada, Y. Sugawa, Role of nitric oxide in pathogenesis of aspirin-induced gastric mucosal damage in rats, Digestion 59 (4) (1998) 298–307, https://doi.org/10.1159/000007506.
[20] P. Holzer, M.A. Pabst, I.T. Lippe, B.M. Peskar, B.A. Peskar, E.H. Livingston, P. H. Guth, Afferent nerve-mediated protection against deep mucosal damage in the rat stomach, Gastroenterology 98 (4) (1990) 838–848, https://doi.org/10.1016/0016-5085(90)90005-l.
[21] R.S. Bresalier, R.S. Sandler, H. Quan, J.A. Bolognese, B. Oxenius, K. Horgan, C. Lines, R. Riddell, D. Morton, A. Lanas, M.A. Konstam, J.A. Baron, Cardiovascular events associated with rofecoxib in a colorectal adenoma chemoprevention trial, New Engl. J. Med. 352 (11) (2005) 1092–1102, https://doi.org/10.1056/NEJMoa050493.
[22] L.A. Garcia Rodriguez, S. Tacconelli, P. Patrignani, Role of dose potency in the prediction of risk of myocardial infarction associated with nonsteroidal anti-inflammatory drugs in the general population, J. Am. Coll. Cardiol. 52 (20) (2008) 1628–1636, https://doi.org/10.1016/j.jacc.2008.08.041.
[23] N.S. Mann, No-Aspirin (NCX 4016), Gastroenterology 125 (6) (2003) 1918–1919, https://doi.org/10.1053/j.gastro.2003.05.015.
[24] J.E. Keeble, P.K. Moore, Pharmacology and potential therapeutic applications of nitric oxide-releasing non-steroidal anti-inflammatory and related nitric oxidedonating drugs, Br. J. Pharmacol. 137 (3) (2002) 295–310, https://doi.org/10. 1038/sj.bjp.0704876.
[25] K. Rehse, F. Brehme, New NO donors with antithrombotic and vasodilating activities, Part 27. Azide oximes and 1-hydroxytetrazoles, Arch. der Pharm. 333(6) (2000) 157–161, https://doi.org/10.1002/1521-4184(20006)333:6 < 157:: aidardp157 > 3.0.co;2-c.
[26] V. Dhawan, D.J. Schwalb, M.J. Shumway, M.C. Warren, R.S. Wexler, I.S. Zemtseva, B.M. Zifcak, D.R. Janero, Selective nitros(yl)ation induced in vivo by a nitric oxide-donating cyclooxygenase-2 inhibitor: a NObonomic analysis, Free Radic. Biol. Med. 39 (9) (2005) 1191–1207, https://doi.org/10.1016/j.freeradbiomed.2005.06.011.
[27] K. Chegaev, L. Lazzarato, P. Tosco, C. Cena, E. Marini, B. Rolando, P.A. Carrupt, R. Fruttero, A. Gasco, NO-donor COX-2 inhibitors. New nitrooxy-substituted 1,5diarylimidazoles endowed with COX-2 inhibitory and vasodilator properties, J. Med. Chem. 50 (7) (2007) 1449–1457, https://doi.org/10.1021/jm0607247.
[28] Y. Shafran, N. Zurgil, O. Ravid-Hermesh, M. Sobolev, E. Afrimzon, Y. Hakuk, A. Shainberg, M. Deutsch, Nitric oxide is cytoprotective to breast cancer spheroids vulnerable to estrogen-induced apoptosis, Oncotarget 8 (65) (2017) 108890–108911.
[29] G.D. Snyder, R.W. Holmes, J.N. Bates, B.J. Van Voorhis, Nitric oxide inhibits aromatase activity: mechanisms of action, J. Steroid Biochem. Mol. Biol. 58 (1) (1996 Apr) 63–69, https://doi.org/10.1016/0960-0760(96)00008-8.
[30] M. Masuda, T. Kubota, S. Karnada, T. Aso, Nitric oxide inhibits steroidogenesis in cultured porcine granulosa cells, Mol. Hum. Reprod. 3 (4) (1997 Apr) 285–292, https://doi.org/10.1093/molehr/3.4.285.
[31] S. Kagabu, H. Kodama, J. Fukuda, A. Karube, M. Murata, T. Tanaka, Inhibitory effects of nitric oxide on the expression and activity of aromatase in human granulosa cells, Molecular Human Reproduction 5 (5) (1999) 396–401, https://doi.org/10.1093/molehr/5.5.396.
[32] K.R.A. Abdellatif, W.A.A. Fadaly, Y. Elshaier, W.A.M. Ali, G.M. Kamel, Non-acidic 1,3,4-trisubstituted-pyrazole derivatives as lonazolac analogs with promising COX-2 selectivity, anti-inflammatory activity and gastric safety profile, Bioorg. Chem. 77 (2018) 568–578, https://doi.org/10.1016/j.bioorg.2018.02.018.
[33] K.R. Abdellatif, W.A.A. Fadaly, W.A. Ali, G.M. Kamel, Synthesis, cyclooxygenase inhibition, anti-inflammatory evaluation and ulcerogenic liability of new

1,5diarylpyrazole derivatives, J. Enzyme Inhib. Med. Chem. 31 (sup3) (2016) 54–60, https://doi.org/10.1080/14756366.2016.1201815.
[34] K.R. Abdellatif, W.A.A. Fadaly, A.A. Azouz, Synthesis, Cyclooxygenase inhibition, anti-inflammatory evaluation, and ulcerogenic liability of new 1,3,5-triarylpyrazoline derivatives possessing a methanesulfonyl pharmacophore, Arch. Pharm. 349 (10) (2016) 801–807, https://doi.org/10.1002/ardp.201600145.
[35] K. R. Abdellatif, Y. Dong, Q. H. Chen, M. A. Chowdhury, E. E. Knaus, Novel (E)-2 (aryl)-3-(4-methanesulfonylphenyl)acrylic ester prodrugs possessing a diazen-1ium-1,2-diolate moiety: design, synthesis, cyclooxygenase inhibition, and nitric oxide release studies, Bioorg. Med. Chem. 15 (21) (2007) 6796–6801, https://doi.org/10.1016/j.bmc.2007.07.021.
[36] K.R. Abdellatif, M.A. Chowdhury, Y. Dong, Q.H. Chen, E.E. Knaus, Diazen-1-ium1,2-diolated and nitrooxyethyl nitric oxide donor ester prodrugs of anti-inflammatory (E)-2-(aryl)-3-(4-methanesulfonylphenyl)acrylic acids: synthesis, cyclooxygenase inhibition, and nitric oxide release studies, Bioorg. Med. Chem. 16 (6) (2008) 3302–3308, https://doi.org/10.1016/j.bmc.2007.12.006.
[37] K.R. Abdellatif, M.A. Chowdhury, Y. Dong, E.E. Knaus, Diazen-1-ium-1,2-diolated nitric oxide donor ester prodrugs of 1-(4-methanesulfonylphenyl)-5-aryl-1H-pyrazol-3-carboxylic acids: synthesis, nitric oxide release studies and anti-inflammatory activities, Bioorg. Med. Chem. 16 (13) (2008) 6528–6534, https://doi.org/10.1016/j.bmc.2008.05.028.
[38] W.A.A. Fadaly, Y.A.M.M. Elshaier, E.H.M. Hassanein, K.R.A. Abdellatif, New 1,2,4-triazole/pyrazole hybrids linked to oxime moiety as nitric oxide donor celecoxib analogs: Synthesis, cyclooxygenase inhibition antiinflammatory, ulcerogenicity, anti-proliferative activities, apoptosis, molecular modeling and nitric oxide release studies, Bioorg. Chem. 98 (2020), 103752, https://doi.org/10.1016/j.bioorg.2020.103752.
[39] K.R. Abdellatif, W.A.A. Fadaly, Y.A. Mostafa, D.M. Zaher, H.A. Omar, Thiohydantoin derivatives incorporating a pyrazole core: Design, synthesis and biological evaluation as dual inhibitors of topoisomerase-I and cycloxygenase-2 with anti-cancer and anti-inflammatory activities, Bioorg. Chem. 91 (2019), 103132.
[40] D. Priya, P. Gopinath, L.S. Dhivya, A. Vijaybabu, M. Haritha, S. Palaniappan, M. K. Kathiravan, Structural insights into pyrazoles as agents against anti-inflammatory and related disorders, ChemistrySelect 7 (2022) e202104429.
[41] A.M. Hussein, A.A. Khames, A.A. El-Adasy, A.A. Atalla, M. Abdel-Rady, M.I. A. Hassan, M.T.M. Nemr, Y.A.A.M. Elshaier, Design, synthesis and biological evaluation of new 2-aminothiazole scaffolds as phosphodiesterase type 5 regulators and COX-1/COX-2 inhibitors, RSC Adv. 10 (2020) 29723–29736.
[42] M.T.M. Nemr, A.M. AboulMagd, New fused pyrimidine derivatives with anticancer activity: synthesis, topoisomerase II inhibition, apoptotic inducing activity and molecular modeling study, Bioorg. Chem. 103 (2020), 104134.
[43] M.T.M. Nemr, A. Sonousi, A.A. Marzouk, Design, synthesis and antiproliferative evaluation of new tricyclic fused thiazolopyrimidines targeting topoisomerase II: molecular docking and apoptosis inducing activity, Bioorg. Chem. 105 (2020), 104446.
[44] M.T.M. Nemr, A.M. AboulMagd, H.M. Hassan, A.A. Hamed, M.I.A. Hamed, M. T. Elsaadi, Design, synthesis and mechanistic study of new benzenesulfonamide derivatives as anticancer and antimicrobial agents via carbonic anhydrase IX inhibition, RSC Adv. 11 (2021) 26241–26257.
[45] M.T.M. Nemr, M.I. Teleb, A.M. AboulMagd, M.E. El-Naggar, N. Gouda, A.A. Abdel-Ghany, Y.A.M.M. Elshaier, Design, synthesis and chemoinformatic studies of new thiazolopyrimidine derivatives as potent anticancer agents via phosphodiesterase-5 inhibition and apoptotic inducing activity, J. Molecular struct. (2022).
[46] R. M. J. J. o. T. B. Botting, Cyclooxygenase: past, present and future. A tribute to John R. Vane (1927–2004), 31(1-2) (2006) 208-219, 10.1016/j.jtherbio.2005.11.008.
[47] J. Naesdal, K. Brown, NSAID-associated adverse effects and acid control aids to prevent them: a review of current treatment options, Drug Saf. 29 (2) (2006) 119–132, https://doi.org/10.2165/00002018-200629020-00002.
[48] M.J. Naim, M.J. Alam, S. Ahmad, F. Nawaz, N. Shrivastava, M. Sahu, O. Alam, Therapeutic journey of 2,4-thiazolidinediones as a versatile scaffold: an insight into structure activity relationship, Eur. J. Med. Chem. 129 (2017) 218–250, https://doi.org/10.1016/j.ejmech.2017.02.031.
[49] B. Cryer, NSAID-associated deaths: the rise and fall of NSAID-associated GI mortality, Am. J. Gastroenterol. 100 (8) (2005) 1694–1695, https://doi.org/10.1111/j.1572-0241.2005.50565.x.
[50] M. Lazzaroni, G. Bianchi Porro, Gastrointestinal side-effects of traditional nonsteroidal anti-inflammatory drugs and new formulations, Aliment. Pharmacol. Therapeut., 20 (Suppl 2) (2004) 48–58, 10.1111/j.1365-2036. 2004.02037.x.
[51] M.W. James, C.J. Hawkey, Assessment of non-steroidal anti-inflammatory drug (NSAID) damage in the human gastrointestinal tract, Br. J. Clin. Pharmacol. 56 (2) (2003) 146–155, https://doi.org/10.1046/j.1365-2125.2003.01934.x.
[52] V. Schneider, L.E. Levesque, B. Zhang, T. Hutchinson, J.M. Brophy, Association of selective and conventional nonsteroidal anti-inflammatory drugs with acute renal failure: a population-based, nested case-control analysis, Am. J. Epidemiol. 164 (9) (2006) 881–889, https://doi.org/10.1093/aje/kwj331.
[53] G. Mounier, C. Guy, F. Berthoux, M.N. Beyens, M. Ratrema, M. Ollagnier, Severe renal adverse events with arylcarboxylic non-steroidal anti-inflammatory drugs: results of a eight-year French national survey, Therapie 61 (3) (2006) 255–266.
[54] J. Zadrazil, Nonsteroidal anti-inflammatory drugs and the kidney, Vnitr. Lek. 52 (7–8) (2006) 686–690.
[55] D. Adebayo, I. Bjarnason, Is non-steroidal anti-inflammaory drug (NSAID) enteropathy clinically more important than NSAID gastropathy? Postgrad. Med. J. 82 (965) (2006) 186–191, https://doi.org/10.1136/pgmj.2005.039586.
[56] D. Clemett, K.L. Goa, Celecoxib: a review of its use in osteoarthritis, rheumatoid arthritis and acute pain, Drugs 59 (4) (2000) 957–980, https://doi.org/10.2165/00003495-200059040-00017.
[57] C. Patrono, P. Patrignani, L.A. Garcia Rodriguez, Cyclooxygenase-selective inhibition of prostanoid formation: transducing biochemical selectivity into clinical read-outs, J. Clin. Investig. 108 (1) (2001) 7–13, https://doi.org/10.1172/jci13418.
[58] Y.A.M.M. Elshaier, M.T.M. Nemr, M. Al Refaey, W.A.A. Fadaly, A. Barakat, Chemistry of 2-Vinylindoles: synthesis and applications, New J. Chem. 46 (2022) 13383–13400, https://doi.org/10.1039/D2NJ00460G.
[59] K.R.A. Abdellatif, W.A.A. Fadaly, G.M. Kamel, Y.A.M.M. Elshaier, M.A. El-Magd, Design, synthesis, modeling studies and biological evaluation of thiazolidine derivatives containing pyrazole core as potential anti-diabetic PPAR-γ agonists and anti-inflammatory COX-2 selective inhibitors, Bioorg. Chem. 82 (2019) 568–578, https://doi.org/10.1016/j.bioorg.2018.09.034.
[60] K.R.A. Abdellatif, A. Moawad, E.E. Knaus, Synthesis of new 1-(4-methane(amino) sulfonylphenyl)-5-(4-substituted-aminomethylphenyl)-3-trifluoromethyl-1H-pyrazoles: Asearch for novel nitric oxide donor anti-inflammatory agents, Bioorg. & Medicinal, Chem. Lett. 24 (2014) 5015–5021, https://doi.org/10.1016/j.bmcl.2014.09.024.
[61] T. Mosmann, Rapid colorimetric assay for cellular growth and survival: application to proliferation and cytotoxicity assays, J. Immunol. Methods 65 (1983) 55–63, https://doi.org/10.1016/0022-1759(83)90303-4.
[62] J.L. Wang, D. Limburg, M.J. Graneto, J. Springer, J.R. Hamper, S. Liao, J. L. Pawlitz, R.G. Kurumbail, T. Maziasz, J.J. Talley, J.R. Kiefer, J. Carter, The novel benzopyran class of selective cyclooxygenase-2 inhibitors. Part 2: The second clinical candidate having a shorter and favorable human half-life, Bioorg. Med. Chem. Lett. 20 (2010) 7159–7163.
[63] A.R. Chopade, F.J. Sayyad, Y.V. Pore, Molecular Docking Studies of Phytocompounds from the Phyllanthus Species as Potential Chronic Pain Modulators, Sci. Pharm. 83 (2) (2014 Nov 8) 243–267, https://doi.org/10.3797/scipharm.1408-10. PMID: 26839814; PMCID: PMC4727797.
[64] L.W.L. Woo, T. Jackson, A. Putey, G. Cozier, P. Leonard, K.R. Acharya, S. K. Chander, A. Purohit, M.J. Reed, B.V.L. Potter, Highly Potent first examples of dual aromatase-steroid sulfatase inhibitors based on a biphenyl template, J. Med. Chem. 53 (2010) 2155.
[65] T.S. Grant, J.A. Mosyak, L. Nicholls, A. Rush, A Shape-Based 3-D scaffold hopping method and its application to a bacterial protein−protein interaction, J. Med. Chem. 48 (2005) 1489.
[66] J. Venhorst, S. Nunez, J.W. Terpstra, C.G. Kruse, Assessment of scaffold hopping efficiency by use of molecular interaction fingerprints, J. Med. Chem. 51 (2008) 3222.
[67] M.A.A. Fayed, M.F. El-Behairy, I.A. Abdallah, H.M. Abdel-Bar, H. Elimam, A. Mostafa, Y. Moatasim, K.A.M. Abouzid, Y.A.M.M. Elshaier, Structure- and ligand-based in silico studies towards the repurposing of marine bioactive compounds to target SARS-CoV-2, Arabian J. Chem. 14 (4) (2021), 103092, https://doi.org/10.1016/j.arabjc.2021.103092.
[68] M.R. Boyd, K.D. Paull, Some practical considerations and applications of the national cancer institute in vitro anticancer drug discovery screen, Drug Dev. Res. 34 (1995) 91–109, https://doi.org/10.1002/ddr.430340203.
[69] M.R. Grever, S.A. Schepartz, B.A. Chabner, The National Cancer Institute: cancer drug discovery and development program, Semin. Oncol. 19 (1992) 622–638.
[70] M.C. Alley, D.A. Scudiero, A. Monks, M.L. Hursey, M.J. Czerwinski, D.L. Fine, B. J. Abbott, J.G. Mayo, R.H. Shoemaker, M.R. Boyd, Feasibility of drug screening with panels of human tumor cell lines using a microculture tetrazolium assay, Cancer Res. 48 (1988) 589.
[71] D.T. Vistica, P. Skehan, D. Scudiero, A. Monks, A. Pittman, M.R. Boyd, Tetrazolium-based assays for cellular viability: a critical examination of selected parameters affecting formazan production, Cancer Res. 51 (1991) 2515–2520.
[72] M.F. Tolba, A. Esmat, A.M. Al-Abd, S.S. Azab, A.E. Khalifa, H.A. Mosli, S.Z. Abdel-Rahman, A.B. Abdel-Naim, Caffeic acid phenethyl ester synergistically enhances docetaxel and paclitaxel cytotoxicity in prostate cancer cells, IUBMB life 65 (2013) 716–729, https://doi.org/10.1002/iub.1188.
[73] D. A. Wink, L. A. Ridnour, S. P. Hussain, C. C. Harris, The reemergence of nitric oxide and cancer, Nitric Oxide: Biol. Chem. 19 (2) (2008) 65–67, https://doi.org/10. 1016/j.niox.2008.05.003.